

---

Masters Theses

Student Theses and Dissertations

---

Fall 2007

## Physical analysis of human hair

Lea Marie Dankers

Follow this and additional works at: [https://scholarsmine.mst.edu/masters\\_theses](https://scholarsmine.mst.edu/masters_theses)

 Part of the [Chemistry Commons](#)

Department:

---

### Recommended Citation

Dankers, Lea Marie, "Physical analysis of human hair" (2007). *Masters Theses*. 6772.  
[https://scholarsmine.mst.edu/masters\\_theses/6772](https://scholarsmine.mst.edu/masters_theses/6772)

This thesis is brought to you by Scholars' Mine, a service of the Missouri S&T Library and Learning Resources. This work is protected by U. S. Copyright Law. Unauthorized use including reproduction for redistribution requires the permission of the copyright holder. For more information, please contact [scholarsmine@mst.edu](mailto:scholarsmine@mst.edu).



PHYSICAL ANALYSIS

OF

HUMAN HAIR

by

LEA MARIE DANKERS

A THESIS

Presented to the Faculty of the Graduate School of the

UNIVERSITY OF MISSOURI-ROLLA

In Partial Fulfillment of the Requirements for the Degree

MASTER OF SCIENCE IN CHEMISTRY

2007

Approved by

---

Frank D. Blum, Advisor

---

Nuran Ercal

---

F. Scott Miller



## ABSTRACT

Physical analysis of human hair has been performed to determine the effects of chemical treatments on hair samples. Five samples including an untreated sample were analyzed using various methods. The methods included differential scanning calorimetry (DSC), thermogravimetric analysis (TGA), Fourier transform infrared spectroscopy (FTIR), and carbon-13 cross polarization/magic-angle spinning nuclear magnetic resonance ( $^{13}\text{C}$  CP/MAS NMR). DSC was only used to analyze untreated hair and endothermic peaks characteristic of hair were easily observed. TGA analysis showed that the treated samples lost mass more gradually with temperature than untreated hair in the range of 500 – 600 °C, suggesting the treatments affected the hair structure. Small differences were observed in the FTIR of the hair samples, when comparing treated to untreated, due to small amounts of environmental damage to the control sample. However, some peak variations suggest more damage to particular samples. The  $^{13}\text{C}$  CP/MAS NMR results showed differences in the shape of the carbonyl resonance for some samples suggesting that  $\alpha$ -helical structures in hair were converted to random coil structures. Slight variations in the aliphatic, methine, and aromatic peaks were also observed between the samples from the CP/MAS experiments.

## ACKNOWLEDGMENTS

I would like to thank my advisor, Frank D. Blum, for his mentoring and support throughout my graduate school experience. Without his wisdom and patience this thesis would not have been possible.

I would also like to thank my committee members, Nuran Ercal and F. Scott Miller for their support. I would like to give a big acknowledgment to the past and present group members who have spent so much time helping me with instruments and giving me advice. Also, the technical help and sample donation of Tadashi Tokuhira helped the research as well.

I would especially like to thank my family and friends who have always been there to support me through my life and encouraged me more than ever through graduate school.

## TABLE OF CONTENTS

	Page
ABSTRACT .....	<b>Error! Bookmark not defined.</b>
ACKNOWLEDGMENTS .....	iv
LIST OF ILLUSTRATIONS .....	vii
LIST OF TABLES .....	ix
SECTION	
1. INTRODUCTION .....	<b>Error! Bookmark not defined.</b>
2. BACKGROUND .....	2
2.1. HAIR STRUCTURE AND COMPOSITION .....	2
2.2. METHODS OF CHARACTERIZATION .....	4
2.2.1. Differential Scanning Calorimetry (DSC).....	5
2.2.2. Thermogravimetric Analysis (TGA) .....	5
2.2.3. Fourier Transform Infrared Spectroscopy (FTIR).....	6
2.2.4. <sup>13</sup> C Cross Polarization/Magic Angle Spin Nuclear Magnetic Resonance (CP/MAS NMR) .....	6
2.3. PREVIOUS STUDIES.....	8
2.3.1. Differential Scanning Calorimetry (DSC).....	8
2.3.2. Thermogravimetric Analysis (TGA) .....	10
2.3.3. Fourier Transform Infrared Spectroscopy (FTIR).....	11
2.3.4. <sup>13</sup> C Cross Polarization/Magic Angle Spin Nuclear Magnetic Resonance (CP/MAS NMR) .....	13
3. EXPERIMENTAL .....	16
3.1. DIFFERENTIAL SCANNING CALORIMETRY (DSC) .....	18
3.2. THERMOGRAVIMETRIC ANALYSIS (TGA) .....	19
3.3. FOURIER TRANSFORM INFRARED SPECTROSCOPY (FTIR) .....	20
3.4. <sup>13</sup> C CROSS POLARIZATION/MAGIC ANGLE SPIN (CP/MAS) NMR.....	20
4.RESULTS.....	24
4.1. DIFFERENTIAL SCANNING CALORIMETRY (DSC) .....	24
4.2. THERMOGRAVIMETRIC ANALYSIS (TGA) .....	24

4.3. FOURIER TRANSFORM INFRARED SPECTROSCOPY (FTIR) .....	35
4.4. <sup>13</sup> C CROSS POLARIZATION/MAGIC ANGLE SPIN (CP/MAS) NMR.....	37
5. DISCUSSION .....	71
5.1. DIFFERENTIAL SCANNING CALORIMETRY (DSC) .....	71
5.2. THERMOGRAVIMETRIC ANALYSIS (TGA) .....	73
5.3. FOURIER TRANSFORM INFRARED SPECTROSCOPY (FTIR) .....	75
5.4. <sup>13</sup> C CROSS POLARIZATION/MAGIC ANGLE SPIN (CP/MAS) NMR.....	76
6. CONCLUSIONS .....	81
BIBLIOGRAPHY .....	83
VITA .....	86

## LIST OF ILLUSTRATIONS

Figure	Page
2.1. Diagram of the three basic layers of hair.....	2
2.2. $^{13}\text{C}$ CP/MAS spectra of PMMA.....	7
3.1. Pulse sequence for standard $^{13}\text{C}$ CP/MAS NMR experiment.....	21
3.2. Pulse sequence for a TOSS $^{13}\text{C}$ CP/MAS NMR experiment.....	21
3.3. Pulse sequence for a DD TOSS $^{13}\text{C}$ CP/MAS experiment.....	22
4.1. DSC curves for untreated hair and water.....	25
4.2. TGA curves for treatments A-E.....	26
4.3. TGA of sample C ramped at 20 °C per minute.....	28
4.4. TGA of samples A-C from lot 2.....	29
4.5. TGA of A-E from lot 1 ramped at 5 °C per minute.....	30
4.6. TGA comparing heating rates of 5 °C and 20 °C per minute with sample A.....	32
4.7. TGA of hair of various chopped lengths.....	33
4.8. TGA of treatment B from two different individuals.....	34
4.9. FTIR spectra of samples A-E.....	36
4.10. Standard $^{13}\text{C}$ CP/MAS NMR spectra of sample A with 7 mm probe.....	39
4.11. Standard $^{13}\text{C}$ CP/MAS NMR spectra of sample B with 7 mm probe.....	40
4.12. Standard $^{13}\text{C}$ CP/MAS NMR spectra of sample C with 7 mm probe.....	41
4.13. Standard $^{13}\text{C}$ CP/MAS NMR spectra of sample D with 7 mm probe.....	42
4.14. Standard $^{13}\text{C}$ CP/MAS NMR spectra of sample E with 7 mm probe.....	43
4.15. Standard $^{13}\text{C}$ CP/MAS NMR spectra of all samples (A – E) with 7 mm probe.....	44
4.16. TOSS $^{13}\text{C}$ CP/MAS NMR spectra of sample A.....	46
4.17. TOSS $^{13}\text{C}$ CP/MAS NMR spectra of sample B.....	47
4.18. TOSS $^{13}\text{C}$ CP/MAS NMR spectra of sample C.....	48
4.19. TOSS $^{13}\text{C}$ CP/MAS NMR spectra of sample D.....	49
4.20. TOSS $^{13}\text{C}$ CP/MAS NMR spectra of sample E.....	50
4.21. TOSS $^{13}\text{C}$ CP/MAS NMR spectra of all samples (A - E).....	51
4.22. DD TOSS $^{13}\text{C}$ CP/MAS NMR spectra of sample A.....	53
4.23. DD TOSS $^{13}\text{C}$ CP/MAS NMR spectra of sample B.....	54

4.24. DD TOSS $^{13}\text{C}$ CP/MAS NMR spectra of sample C .....	55
4.25. DD TOSS $^{13}\text{C}$ CP/MAS NMR spectra of sample D .....	56
4.26. DD TOSS $^{13}\text{C}$ CP/MAS NMR spectra of samples (A - D).....	57
4.27. Comparison of the 3 NMR experiments using sample B .....	58
4.28. Standard $^{13}\text{C}$ CP/MAS NMR spectra of sample A with 5 mm probe .....	59
4.29. Standard $^{13}\text{C}$ CP/MAS NMR spectra of sample B with 5 mm probe .....	60
4.30. Standard $^{13}\text{C}$ CP/MAS NMR spectra of sample C with 5 mm probe .....	61
4.31. Standard $^{13}\text{C}$ CP/MAS NMR spectra of sample D with 5 mm probe .....	62
4.32. Standard $^{13}\text{C}$ CP/MAS NMR spectra of sample E with 5 mm probe .....	63
4.33. Standard $^{13}\text{C}$ CP/MAS NMR spectra of all samples (A-E) with 5 mm probe.....	64
4.34. Standard $^{13}\text{C}$ CP/MAS NMR spectra of sample E with 5 mm probe NO MAS .....	67
4.35. Comparison of sample E with and without MAS .....	68
4.36. Comparison of 5 mm and 7 mm probe with sample E .....	69
4.37. Standard $^{13}\text{C}$ CP/MAS NMR spectra of burnt hair .....	70
5.1. Close comparison of the carbonyl peaks for all samples .....	79
5.2. Close comparison of the aliphatic and methine peaks for all samples .....	80

**LIST OF TABLES**

Table	Page
2.1. Typical amino acid analysis of human hair. ....	<b>Error! Bookmark not defined.</b>
3.1. Summary of the treatments used.....	17
3.2. The spinning speeds in kHz of each experiment using the 7 mm probe.....	23
3.3. The spinning speeds in kHz of each experiment using the 5 mm probe.....	23
4.1. Peak assignments for the FTIR of hair .....	37
4.2. Peak assignments for the <sup>13</sup> C CP/MAS of hair .....	38

## 1. INTRODUCTION

Hair treatments are commonly used to obtain a desired look, shape, or texture. However, treatments can cause damage to the hair on a molecular level which can make the outward appearance look or feel unnatural or undesirable. An ideal treatment would perform a task, such as creating a particular style, with minimal molecular damage to the hair. To develop improved treatment formulas or methods, a better understanding of what happens to the hair on the molecular level as a result of hair treatments is necessary.

Common hair treatments include reducing hair for permanent waving or relaxing, and oxidizing for bleaching or dying. A permanent wave or relaxing treatment reduces the cystine disulfide bond, forming byproducts of sulfur bonded to the reducing agent or cystine with the reducing agent. Bleaching and dying treatments usually oxidize cystine and other amino acids in hair producing products such as cystine mono-, di-, tri-, and tetra- oxide as well as sulfonates. As a result of both treatments, a decrease in the amount of cystine is observed by amino acid analysis (Robbins, 2002).

Five samples, all from the same individual, including an untreated sample have been analyzed. A comparison of the five samples has been made using differential scanning calorimetry (DSC), thermogravimetric analysis (TGA), Fourier transform infrared spectroscopy (FTIR), and  $^{13}\text{C}$  cross polarization/magic angle spin nuclear magnetic resonance ( $^{13}\text{C}$  CP/MAS NMR) to understand how each of the treatments affects the hair on the molecular level. In addition, the reproducibility of TGA results was performed using three hair samples from the same person, but a different individual than the one whom the first five samples were from.

## 2. BACKGROUND

### 2.1. HAIR STRUCTURE AND COMPOSITION

Human hair is primarily composed of three layers: the cuticle, cortex, and medulla. Figure 2.1 shows a simple diagram of those three layers. Keratin, which is a strong protein, is dispersed throughout the hair matrix, giving the hair strength. The cuticle functions as a protective outer layer. The cortex has the largest mass of the three layers and contains spindle shaped cells that run along the hair fiber. The center-most layer is the medulla which contains amino acids responsible for hair color (these amino acids are also found dispersed in the cortex). All of the layers are held together by the cell membrane complex (Robbins, 2002).

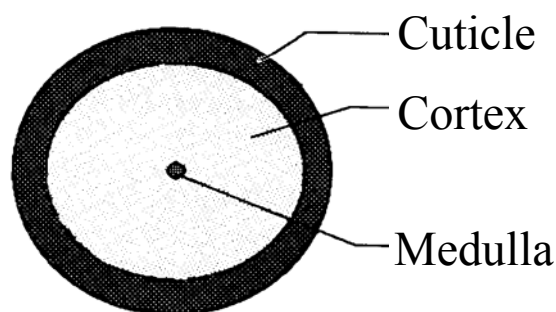


**Figure 2.1.** Diagram of the three basic layers of hair. The cuticle is on the outside, the cortex is the next layer in, and the medulla is in the very center. From: Robbins, Clarence R., *Chemical and Physical Behavior of Human Hair 4th Ed.*, Springer, New York, 2002.

As stated above, the cuticle is a protective layer on the outer-most surface of the hair. It covers the hair in scale-like fashion, providing protection from weather, brushing, and chemical treatment. Each cuticle cell can be broken down into different layers. The outer-most layer is the epicuticle with a thickness of 50-100 Å. The epicuticle is thought to consist of approximately 75% heavily cross-linked protein and 25% fatty acids (mostly 18-methyleicosanoic acid). The next layer is the A layer which has a high level of cystine (>30%) and is therefore a resilient protective layer. The next layer in is the exocuticle (or B layer) which has a ~15% cystine content. Finally, the endocuticle containing a ~3% cystine content is found.

The cortex is the next layer and is the major, by mass or volume, portion of hair. Cortical cells run lengthwise through the hair and are approximately 1-6  $\mu\text{m}$  thick and 100  $\mu\text{m}$  long. The cortical cells are held together with the cell membrane complex. Each cortical cell is made up of macrofibrils which contain microfibrils. The diameter of each macrofibril is approximately 4000  $\text{\AA}$  and each microfibril is around 75  $\text{\AA}$ . The microfibrils consist of chains of polypeptide protein. These chains are about 10  $\text{\AA}$  in diameter and are found in  $\alpha$ -helix formation. The individual polypeptide chains can be categorized as Type I and Type II which form the helical structure. Type I and Type II vary by their amino acid sequencing. Type I proteins consist of 392-416 amino acids and are slightly acidic, while Type II consists of 479-506 amino acids and are neutral-basic.

The medulla is the inner-most layer of hair. In some cases, the medulla may be absent or sometimes there may be a double medulla. Fine hair typically has little to no medulla, but in thicker, course hair, such as facial hair, the medulla maybe continuous or divided into two layers. Hair pigments, which give the color, are mainly concentrated in the medulla and also the cortex as melanins. Pheomelanins and eumelanins are basically the two types of pigments found in the melanocytes. Pheomelanins are red – yellow color and eumelanins are dark pigments. The ratio between these two pigments determines the hair color (Robbins, 2002).

The cell membrane complex, also know as intercellular matter or nonkeratinous region, is an adhesive material holding all the components of hair together. It is believed that the cell membrane complex is the primary pathway for diffusion of chemical treatments. The complex is a sandwich layered system, with the outer layers being the epicuticle containing crosslinked protein and fatty acids, then the delta layer, or intercellular cement in the middle containing low cystine proteins and high polar amino acids (12% basic and 17% acidic amino acids) (Robbins, 2002).

Amino acid analyses of human hair have been made by several researchers, and, although the quantities and types of amino acids differ slightly between individuals based on diet, the ratios are very similar. Table 2.1 gives an example of the amino acids present in hair and their relative quantities.

<u>Amino Acid</u>	<u>% of Total Residues</u>
Lysine	2.7
Histidine	0.9
Arginine	5.8
Aspartate + Asparagine	4.9
Threonine	6.8
Serine	11.7
Glutamate + Glutamine	11.4
Proline	8.4
Glycine	6.4
Alanine	4.6
Half - Cystine	17.8
Valine	5.8
Methionine	0.6
Isoleucine	2.6
Leucine	5.8
Tyrosine	2
Phenylalanine	1.6
<b>Total</b>	<b>99.8</b>

**Table 2.1.** Typical amino acid analysis of human hair. The analysis varies slightly between individuals. From: Nishikawa, N.; *et al.*, *Polymer J.*, **1998**, *30*, 125.

In most cases, the composition of human hair is mostly half-cystine, serine, and glutamic acid. Half-cystine, accounting for almost 18% of hair, is responsible for a large degree of crosslinking which gives hair strength (Robbins, 2002).

## **2.2. METHODS OF CHARACTERIZATION**

Previous studies of hair have used different methods to analyze the mechanical, physiological, and physical components of hair. Presently, our studies have utilized differential scanning calorimetry (DSC), thermalgravimetric analysis (TGA), Fourier-transform infrared spectroscopy (FTIR), and  $^{13}\text{C}$  cross polarization/magic angle spinning

nuclear magnetic resonance (CP/MAS NMR) to obtain information on thermal stability and physical characteristics. The data obtained from each method was used to compare how the different treatments affected the hair samples.

**2.2.1. Differential Scanning Calorimetry (DSC)** DSC is often used to find the glass transition temperature ( $T_g$ ) of polymers. DSC measures the heat transferred into or out of a sample in comparison to a reference. The DSC cell is composed of two heating compartments, one for the sample and one for reference. Usually the reference pan is left empty. The instrument and computer control the heating so that the temperature of both sample and reference pans are the same. When materials such as polymers undergo a physical or chemical change (such as melting), the heat capacity of the material changes. These changes are monitored by a computer, and to keep the temperature of the two components the same, differential heating is applied to the sample and reference components. For example, a sample going through an endothermic process will be at a lower temperature than the reference, so often heat must be transferred into the sample to maintain both components at the same temperature. This heat transfer is detected by the instrument and a record of it is kept by the computer. A thermogram is produced and usually plotted as heat flow versus temperature. A thermogram for polymers may show slope changes due to  $T_g$ , exothermic peaks due to crystallization ( $T_c$ ), and endothermic peaks due to melting ( $T_m$ ) (Stevens, 1999).

**2.2.2. Thermogravimetric Analysis (TGA)** TGA is used to study the thermal stability of a material. The most common method of TGA is to continuously weigh a sample with a sensitive balance while heating the sample in the presence of air or an inert gas. As the temperature increases, mass loss occurs due to evaporation of water or solvent, decomposition or reaction of the material. The mass measurements are collected over a range of temperatures and processed by a computer. A thermogram is produced which is a plot of mass versus temperature. Mass loss can occur in steps based on the temperature that the material leaves the sample pan. For example, a polymer with residual solvent present may show a mass loss step at lower temperatures due to solvent escaping, then a second step due to the degradation of the polymer. The weight of sample lost at each step can be calculated, thereby giving information on the amount of a particular material in the sample (Stevens, 1999).

**2.2.3. Fourier Transform Infrared Spectroscopy (FTIR)** FTIR is commonly used to identify compounds or the purity of a material. Infrared radiation in the range of 10,000 to 100  $\text{cm}^{-1}$  is used to irradiate a sample. Organic material absorbs and converts the energy to vibrations of the chemical bonds which join the atoms. The wavelengths at which the molecules absorb at depend on the masses of the atoms, the force constants of the bonds, and the geometries of the atoms. Different species in the molecules vibrate and rotate producing bands at particular frequencies (measured in  $\text{cm}^{-1}$ ). The absorption regions for different moieties are generally known, so a spectra produced can be compared to the known values to identify the material. For a general example, C-C, C-O, and C-N absorb between 1300-800  $\text{cm}^{-1}$ , C=O, C=C, C=N, and N=O absorb at 1900-1500  $\text{cm}^{-1}$ , C $\equiv$ C and C $\equiv$ N absorb from 2300-2000  $\text{cm}^{-1}$ , and C-H, O-H, and N-H absorb at 3800-2700  $\text{cm}^{-1}$ . The spectra produced are plotted either % transmittance (%T) or absorbance (A) verses wavenumbers ( $\text{cm}^{-1}$ ) or wavelength ( $\mu\text{m}$ ) (Silverstein et al., 1981).

**2.2.4.  $^{13}\text{C}$  Cross Polarization/Magic Angle Spin Nuclear Magnetic Resonance (CP/MAS NMR)** NMR is a powerful tool used to identify materials. Nuclei with a spin number ( $I$ ) of  $\frac{1}{2}$ , such as  $^1\text{H}$ ,  $^{13}\text{C}$ , and  $^{19}\text{F}$ , or greater are considered magnetically “active” and can yield an NMR signal. In the absence of a magnetic field, nuclei have randomly oriented magnetic moments. In the presence of a magnetic field, the nuclei align, in part, with or against the magnetic field. A radio frequency electromagnetic wave is used to pulse the sample, which perturbs the alignment. After perturbing, the nuclei relax back to alignment, and the resulting signal is known as free induction decay (FID). The FID signal is converted to a frequency domain spectrum using Fourier transform (FT).

Solid state NMR differs from liquid NMR in that the anisotropic interactions are observed, which cause broad peaks. In liquid NMR, the anisotropic interactions are averaged due to random tumbling and narrow resonances are observed. To counteract the broad resonances produced from solid samples, special techniques are used such as cross polarization and magic angle spinning (among others). The technique of cross polarization uses abundant nuclei spins such as  $^1\text{H}$  to enhance non-abundant spins such as  $^{13}\text{C}$ . Cross polarization can increase the signal to noise ratio (S/N) by as much as four times and shorten the  $T_1$  relaxation time. Magic angle spinning can produce narrower resonances. Generally faster spinning results in more useful spectra. The “magic angle”,

along which the sample sits, is roughly  $54^\circ$  from the static magnetic field axis. High power proton decoupling is another technique used to remove dipolar coupling to protons (Fyfe, 1983).

The combination of cross polarization and magic angle spinning along with high power proton decoupling, can produce narrow peaks as shown in Figure 2.2 where an example of poly(methyl methacrylate) (PMMA) is displayed.

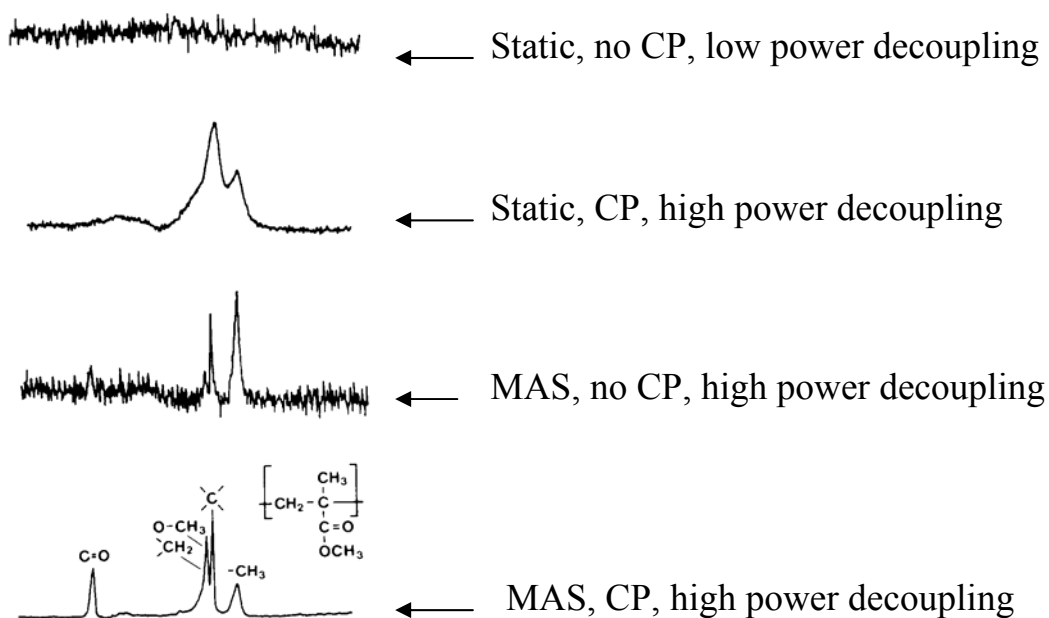


**Figure 2.2.**  $^{13}\text{C}$  CP/MAS spectra of PMMA showing the effect of cross polarization, magic angle spinning, and high power proton decoupling. From: Fyfe, Colin A., *Solid State NMR for Chemists.*, C.F.C Press, Ontario, Canada, 1983.

The top spectrum in Figure 2.2 shows the results of a sample not spinning, with no cross polarization, and low power proton decoupling. The second spectrum illustrates the use of cross polarization and high-power proton decoupling, so resonances are observed with good S/N, however the lines are broad. The third spectrum down shows the use of magic angle spinning so the lines are narrow, but no cross polarization, so the S/N is poor. A combination of all techniques is shown for the last spectrum, where narrow peaks and good S/N is observed (Fyfe, 1983).

## 2.3. PREVIOUS STUDIES

Analyses of human hair have been made for many years using numerous methods and instruments. Most of the research has focused on the hair itself rather than the effects of treatments on human hair. Thermal analysis instruments such as DSCs and TGAs have been used to measure the denaturation or decomposition behavior of both untreated hair and treated hair. FTIR has been previously used to characterize and quantify oxidation of treated hair samples.  $^{13}\text{C}$  CP/MAS NMR has also been used as a tool to characterize hair and to analyze the affect treatments have on hair. While previous work with DSC, TGA, FTIR, and  $^{13}\text{C}$  CP/MAS NMR to study hair and the effect of treatments on hair is fairly limited, several researchers have analyzed other forms of proteins in various environments with these methods. In addition, research has been done to study hair treatments which straighten hair (Caldwell, 1996), along with research focusing on the properties of African American hair when straightened or relaxed (Quadflieg, 2003). The previous research performed and the results of those studies have been useful in analyzing our results and drawing conclusions about the effect that treatments have on human hair.

**2.3.1. Differential Scanning Calorimetry (DSC)** DSC is commonly used to find the  $T_g$  of polymers; however, for hair it has been used to study the thermal stability and morphological phases of hair. Wortmann et al. analyzed Merino wool fibers in water using high pressure (HP) DSC and observed two endothermic peaks at 137.7 °C and 141.7 °C, corresponding to ortho- and para- cortical cells, respectively. The denaturation enthalpies ( $\Delta H$ ) were also measured. The higher temperature at which the para-cells denatured was attributed to a higher concentration of disulfide linkages (or cystine) in the para-cells (Wortmann et al., 1998). Additional work by Wortmann et al. has been done to analyze human hair in water with DSC. The thermogram produced showed only one endothermic peak at 156.7 °C, representing the denaturation. The enthalpy of denaturation was also measured for the single peak at 156.7 °C. It was concluded that the denaturation enthalpy depends on the strength of the intermediate filaments, which are composed of  $\alpha$ -helical proteins. The denaturation temperature is dependant on the crosslink density of the matrix which surrounds the intermediate filaments. Wortmann et al. also looked at the effects of bleaching and permanent waving of hair with DSC. After

excessive bleaching and permanent wave treatments, the temperature of denaturation and denaturation enthalpies were reduced for both types of samples. It was suggested that structural damage from the treatments causes the denaturation to be at a lower temperature and less intense because there was a loss or denaturation of native  $\alpha$ -helical proteins (Wortmann et al., 2002). It was also concluded by Popescu et al. that the bleaching affects the amorphous matrix and  $\alpha$ -helix faster than the permanent wave treatment (Popescu et al., 2003).

Further research by Wortmann et al. used DSC to analyze the glass transition ( $T_g$ ) of human hair and its dependence on the amount of water present during analysis. The Fox equation was used to describe the data, showing that the  $T_g$  of human hair was 144 °C. In contrast, wool exhibited a  $T_g$  of 174 °C, suggesting that human hair contains a higher amount of hydrophobic proteins in the hair matrix which act as a plasticizer. By examining hair in the amorphous state they suggested that water is distributed throughout the  $\alpha$ -keratin of hair (Wortmann et al., 2006).

Other DSC studies have attempted to mimic the environment that hair would be exposed to during drying with a heat source or in curling hair (Milczarek et al., 1992). These experiments used DSC pans which were punctured to allow water to evaporate while heating. DSC curves of hair samples which were dried by annealing at temperatures of 70 °C and higher and samples exposed to 50% humidity were compared to analyze the affect of water on the resulting thermogram. The samples which were stored at 50% humidity exhibited a large endothermic peak at 75 °C, while the annealed samples did not exhibit this peak, which leads to the conclusion that the endothermic peak at 75 °C is due to water. Both samples showed two other transitions, one at 155 °C and an endothermic peak at 233 °C. The transition at 155 °C was attributed to a transition in the amorphous phase, known as the “toughening transition,” and was not a peak, but a change in slope, which was described by the authors as an opposite character of  $T_g$ , meaning the expansion coefficient decreased with temperature. The other process was a peak at 233 °C due to the melting/denaturation of the  $\alpha$ -crystalline phase (Milczarek et al., 1992).

DSC has also been used to analyze hair samples for forensic science purposes. Ionashiro et al. investigated the possibility that DSC analysis could be used to identify

individuals. The project compared different ethnic group's hair samples and also several individuals to produce a data bank. They concluded that it is not possible to detect an individual ethnicity with DSC, but slight variations in the DSC curve among individuals may make it possible to identify a person with a reference sample (Ionashiro et al., 2004).

**2.3.2. Thermal gravimetric analysis (TGA)** TGA measures the thermal stability of a material and has been used to some degree to analyze human hair. Early TGA studies on hair were done by Humphries et al. The experiments compared untreated hair to hair which had been treated by oxidation with  $H_2O_2$ , reduction with thioglycolic acid, crosslinked by formaldehyde vapors, and supercontracted by heating to 95 °C in 8M LiBr. The TGA sample was heated from 30-550 °C and the transition temperature was measured for each sample. The untreated sample showed a transition temperature of 252 °C while the reduced sample had a transition temperature that was slightly less than the untreated sample. They postulated that reducing the hair converts disulfide crosslinks to thiol groups which are less thermally stable. The oxidized, crosslinked, and supercontracted samples all had higher transition temperatures of 270, 276, and 270 °C, respectively. No explanation, on the molecular level, as to why the oxidized hair has a higher transition temperature, but the crosslinked sample may have formed bridges between the polypeptide chains, creating more structural support for the hair. The supercontracted sample causes shortening of the sample resulting in folding of the polypeptide chains. This folding is the apparent reason for the sample being more thermally stable than the untreated samples (Humphries et al., 1972).

Additional research on the thermal stability of hair has coupled DSC with TGA. Monteiro et al. analyzed the effect of bleaching hair and chlorination treatments with DSC and TGA. As with previous research on treated hair with DSC, the denaturation enthalpy decreases due to the increased disorganization of hair structure, primarily keratin. However, the temperature of denaturation stayed almost the same and even slightly increased, in contrast to other research previously described where the denaturation temperature decreased after treatments. This slight increase in denaturation temperature was attributed to reorganization of organic chains after denaturation. However, the increased temperatures were very small and no error limits were given. The TGA results they obtained exhibited more mass loss steps and at lower temperatures

for the untreated hair samples than for the treated samples. They claim this is because hair keratin becomes more disorganized after treatments leading to fewer discernable mass loss stages. The variation in temperature is due to the treatments causing a transformation of the keratin structure and, therefore, treated hair lost mass at higher temperatures compared to untreated hair. The mass loss steps were assigned in the order of water loss first from 25-131 °C, then denaturation of keratin and organic degradation at 280, 320, and 350 °C. The final step is due to the complete degradation of hair keratin around 350-550 °C (Monteiro et al., 2005).

Further investigations into the thermal characterization of hair were done by Éhen et al. Their research compared DSC and TGA curves of human hair to the DSC and TGA curves of common amino acids in hair: aspartic acid, glutamic acid, histidine, and tyrosine. Of the individual amino acids, histidine was the least thermally stable and tyrosine was the most thermally stable. The hair samples they used were from a variety of individuals with different age, gender, and hair color. The DSC and TGA experiments of the hair samples were run from 30-350 °C and all samples had a similar shape. The DSC showed two endothermic peaks, one around 60 °C (the loss of water) and the other around 230 °C (the denaturation of keratin). The TGA curve showed an initial mass loss of water from 30-250 °C and a final mass loss though 350 °C from organic degradation and keratin denaturation. Another important discovery was that the heating rate used for TGA affected the resulting thermogram. With a higher heating rate (50 °C/min), the decomposition was shifted toward higher temperatures by 30 °C compared to the lower heating rate (5 °C/min) while retaining the same general shape (Éhen et al., 2004).

**2.3.3. Fourier Transform Infrared Spectroscopy (FTIR)** Early research performed using infrared spectroscopy (IR) to analyze hair samples was conducted by Alter et al. The oxidation of hair keratin with attenuated total reflectance (ATR) IR was studied. The samples used for comparison were untreated hair and bleached hair (treated with H<sub>2</sub>O<sub>2</sub>) which was treated numerous times. The differences in the IR spectra after bleaching the hair showed an appearance of new peaks at 1175 and 1040 cm<sup>-1</sup>. These peaks were due to sulfonates which are formed by oxidation of cystine. Cystine dioxide peaks, also due to oxidation of cystine, were observed at 1220 and 1310 cm<sup>-1</sup>, appeared and increased in size after successive bleaching (Alter et al., 1969).

IR studies examined the effects that bleaching, thioglycolate waving, bisulfide waving, and weathering have on the disulfide bond in cystine using a diamond cell IR (Strassburger et al., 1985). The results showed that hair waved with bisulfite exhibited the most oxidation, followed by bleached hair, and then thioglycolate waved hair had the least oxidation. Hair samples were also weathered, both treated and untreated, using a weathering machine and also outdoor exposure. Weathered only hair showed small yet measurable amounts of oxidation. Hair that was bleached and weathered showed more oxidative damage than hair that was waved and weathered. An important point made by the researchers is that oxidative damage is mostly concentrated in the cuticle and outer portion of the cortex. This is because the cuticle cells are intended to protect the inner layers of hair so penetration of hair treatments is not usually deep into the hair. It was also observed that hair samples from different portions of the hair (root to tip) exhibited different oxidation levels, with hair from the tip showing the most oxidation. IR does not penetrate the hair fiber, so only the oxidation on the outer layers is observed with this method of analysis. According to Strassburger et al., this particular IR method which utilizes diamond cell FTIR was found to be an effective and reproducible method to determine sulfonate concentrations in hair by using spectral subtraction; however, the coefficient of variation between each measurement was high (Strassburger et al., 1985).

FTIR was also used to study treated and untreated hair samples by Kirschenbaum et al. Their results showed that in addition to disulfide bond breakage, the peptide backbone was affected by chemical treatments. The damaged hair showed increased intensities of C-H peaks, which they suspected corresponded to the structural transformation of  $\alpha$ -helices to  $\beta$ -sheets (Kirschenbaum et al., 2000).

IR research has been carried out by Signori et al. using an ATR diamond cell IR method. They also measured the concentration of oxidative damage of hair due to bleaching by observing the cysteic acid peak variations through spectral subtraction and normalizing, when compared to untreated hair. Although the differences in spectral results were not discussed, the method of obtaining the data was described as an excellent tool for obtaining spectra of hair (Signori et al., 1997). Further discussion of IR methods for hair analysis by Martin compared ATR using ZnS cells and diamond cells. The diamond cells gave the most reproducible results (Martin, 1999). Although the previous

methods have suggested reproducible results to analyze the oxidative damage in hair, IR still poses difficulty of obtaining information about the damage treatments cause to the inside of hair fibers because IR only penetrates the outer position of hair. Micro ATR FTIR, in combination with a focal plane array (FPA) detector, has also been used to study the cross-section of hair fiber (Chan et al., 2005).

Another method of IR has been used to analyze the interior and surface damage of hair in a non-destructive manner. Near-IR diffuse reflectance (NIR-DR) spectroscopy was used to evaluate the damage to both the surface and interior of hair due to chemical treatments by using a fiber probe on the hair and analyzing the samples in the region of  $5060\text{-}4500\text{ cm}^{-1}$ . This method was used to simultaneously monitor the changes of interior proteins as well as the surface of the hair after hair treatments (Miyamae et al., 2006).

Other FTIR studies involving hair include analyzing the hydrogen bonds around hair protein to understand the mechanism of improving the durability of hair-setting with a certain treatment (Itou et al., 2006), and also studying isolated melanins from fair, red and dark hair (Bilinska et al., 1991). IR has also been used to study protein sources other than human hair, such as horse hair (Lyman et al., 2000), plant cutin (Benitez et al., 2004), along with human skin, nails, and lipids (Gniadecka et al., 1998). A different role of IR in the area of hair care has utilized an IR light source to apply a polymer coating or film on hair fibers to act as a protective layer. The IR irradiation increases the polymer's molecular weight, giving better performance (Witteler et al., 2001; Morinaga et al., 2006).

**2.3.4.  $^{13}\text{C}$  Cross Polarization/Magic Angle Spin Nuclear Magnetic Resonance (CP/MAS NMR)** Several studies have used  $^{13}\text{C}$  CP/MAS NMR so study human hair and other forms of proteins. A lot of research has been done by Nishikawa et al. using NMR to analyze human hair. One study looked at the keratin intermediate filament (a.k.a. microfibrils) portion of hair samples which is made up of  $\alpha$ -helical structures. These intermediate filaments, which are low in sulfur, were extracted from the hair and then exposed to various pH levels, ranging from 5.0 to 9.6 pH. The varying pH exposures were intended to mimic hair treatments such as bleaching or permanent waving. The theory behind this analysis is that hair treatments cause a change in mobility of the  $\alpha$ -helical rod-like structures therefore changing the mechanical properties of hair. The

samples were prepared as a liquid sample with D<sub>2</sub>O as the solvent and <sup>13</sup>C NMR was used to study the affect of the different pH exposures. With decreasing pH, the intensity of the resonances decreased. Nishikawa et al. was also able to provide detailed assignments of the spectra (Nishikawa et al., 1998 – b).

Nishikawa et al. also studied human hair with <sup>13</sup>C CP/MAS NMR. This study compared the spectra of untreated hair and hair which was exposed to permanent waving. Variations in the spectra were observed between the samples for all the peaks. The carbonyl peak exhibited the most change and was used for close comparison. The top of the carbonyl peak of the untreated hair was tilted slightly to the right (lower frequency) and a small hump was visible to the left (higher frequency). After successive treatments of up to 180 minutes exposure time, the small hump at higher frequency was gone, although the peak remained tilted toward lower frequency. The carbonyl peak is made up of side chain carbonyl peak at 180 ppm, the small hump at 176 ppm is  $\alpha$ -helical proteins, and the larger hump at lower frequency is a combination of random coils and  $\beta$ -sheet structure proteins. It was concluded that the treatments were causing  $\alpha$ -helical proteins to convert to random coils, therefore decreasing the hump at higher frequency (Nishikawa et al., 1998 – a).

Additional <sup>13</sup>C CP/MAS NMR research was performed by Yoshimizu et al. where untreated hair samples were compared to hair which was stretched to different degrees and also hair which was heated. Both the carbonyl and aliphatic peaks were observed for changes. The results indicated that stretching hair by 200 and 300% decreased the amount of  $\alpha$ -helical structures while increasing the amount of  $\beta$ -sheet structures. This was observable with the carbonyl peak where the peak at 176 ppm ( $\alpha$ -helical structures) decreased and the peak at 172 ppm (mainly  $\beta$ -sheet structures) increased. Small differences were observed between the samples in the aliphatic region indicating coiled structures observable in the aliphatic region maintained their shape after stretching. The effect of heating a hair sample to 200 °C for 3 hours was also analyzed. The overall appearance of both the carbonyl and aliphatic peaks were broader than the unexposed sample. Their conclusion was that some random coiled structures appear after heating, yet a large amount of  $\alpha$ -helical structures do not change (Yoshimizu et al., 1991).

Other studies of human hair using NMR include determination of the relaxation times  $T_1$  and  $T_2$  of water protons in hair (Clifford et al., 1966), structural and chemical comparison of black and red human hair melanin samples with  $^{13}\text{C}$  CP/MAS (Liu et al., 2005), and melanin comparisons using samples from human hair and *Sepia* melanin (from cuttlefish) analyzed with  $^{15}\text{N}$  and  $^{13}\text{C}$  CP/MAS (Ahyaru et al., 2003). Analysis of protein from various sources has also been performed using CP/MAS NMR. Individual amino acids (Derome et al., 1991), polypeptide sequences (Smith et al., 1988), and natural polymers from materials such as lignin, wood, silk protein, and chitin (Lindberg et al., 1986) have all been analyzed using CP/MAS NMR. These studies have given insight into the molecular structure and spectral assignment of more complex proteins.

### 3. EXPERIMENTAL

Hair samples were obtained from an African American subject. All five samples were from the head of one African American subject, a 2.5 year old male, and included one control and four with different treatments. The samples were chopped to an approximate length of 1-2 mm and in quantities of 60-70 mg. In addition to the treated samples, 6 g of untreated Caucasian hair was obtained for practicing analysis techniques. All samples were kept in vials at room temperature (25 °C) and relative humidity of roughly 35%. An additional set of 3 hair samples (including an untreated sample) was obtained, denoted lot 2 whereas the initial set of 5 samples is denoted lot 1. The samples from lot 2 are from a different African American subject than from lot 1, a 24 year old male. All three samples in lot 2 are from the same subject. Unless specified, all analysis was performed using lot 1 samples.

Prior to treatment or analysis, all hair samples were cleaned and tested with an amino acid analyzer to look for excess oxidation or lanthionization and to confirm that the hair was untreated. The cleaning procedure started by prewetting the hair with water at 40 °C. The hair was then exposed to a 10% solution of ammonium lauryl sulfate, 4 mL of solution for every gram of hair, and the solution was massaged into hair for 1 minute. The hair was rinsed with 40 °C water and dried with a blotting action. The samples were allowed to equilibrate at 25 °C and 45% relative humidity for at least 8 hours in an environmental chamber. Following the cleaning and oxidation testing, the hair samples were treated. Treatments included ammonium thioglycolate, sodium hydroxide, guanidine hydroxide, and bleaching. An untreated sample was set aside for comparison analysis. The treatments were labeled A-E during the testing process. A summary of the treatments and the labeling used to identify is shown in Table 3.1. Samples A-E were obtained as lot 1 and samples A-C were obtained as lot 2.

<u>Treatment</u>	<u>Labeled – Lot 1</u>	<u>Labeled – Lot 2</u>
untreated	A	A
ammonium thioglycolate	B	B
sodium hydroxide	C	C
guanidine hydroxide	D	N/A
bleaching	E	N/A

**Table 3.1.** A summary of the treatments used and the labeling used to identify them during analysis.

Ammonium thioglycolate is commonly used in permanent curling hair and can also be used to relax the curl in hair. Thioglycolate is a reducing agent which reduces the disulfide cystine bond in the hair cortex. Reducing is followed by oxidation, usually with hydrogen peroxide, to reform the disulfide bond. Ammonium helps the thioglycolate diffuse into the cortex by swelling the hair. The pH of a typical solution is usually 9 to 9.5. Ammonium thioglycolate is thought to be a better alternative to sodium hydroxide or guanidine hydroxide for relaxing hair because it is less aggressive.

Sodium hydroxide (a.k.a. lye) is the most common relaxant of hair, and has a pH that can range from 10 to 14. The sodium hydroxide solution works similarly to the ammonium thioglycolate by penetrating to the cortex then breaking the disulfide cystine bond. Sodium hydroxide is commonly found in drain cleaners because of its ability to breakdown hair proteins.

Guanidine hydroxide, similar to sodium hydroxide because of the hydroxide technologies, but it is a mixture of guanidine carbonate as an activator and calcium hydroxide cream. This treatment requires before and after conditioning treatments because it de-fats the scalp. Prior to treating the hair with guanidine hydroxide, a scalp protector is applied which is a petroleum based substance with high water repellence.

Bleaching hair is done with a mixture of several components, the primary chemical being hydrogen peroxide. The objective of bleaching is to oxidize the hair pigments which lighten the color. During this oxidation process, other proteins in the

hair are also oxidized which leads to cell membrane damage causing the cortex and cuticle to separate. Hydrogen peroxide is used because it oxidizes the melanin faster than it oxidizes the other proteins in hair so color lightening can be achieved faster to prevent too much damage (Robbins, 2002).

The samples were analyzed using differential scanning calorimetry (DSC), thermal gravimetric analysis (TGA), Fourier transform infrared spectroscopy (FTIR), and cross polarization/magic angle spinning (CP/MAS)  $^{13}\text{C}$  NMR. DSC is commonly used to measure the thermal transitions of a material by monitoring the heat flow going into and out of a sample over a range of temperatures compared to a reference. TGA measures the thermal stability of a material by heating the sample and measuring the mass loss at a given temperature. FTIR is commonly used to identify compounds by irradiating samples with infrared light and observing loss of incidental radiation due to the molecular vibrations, which produces a spectrum. NMR is also commonly used to identify compounds, among other uses. CP/MAS solid state NMR has advantages over traditional solid state NMR. The cross polarization uses abundant spins, usually  $^1\text{H}$ , to enhance non-abundant spins, usually  $^{13}\text{C}$ . This technique also increases S/N by about four times and decreases the time between scans. Magic angle spinning narrows lines. In general, the faster the spinning the narrower the resonances. High power proton decoupling is also used to remove dipolar coupling to protons.

### **3.1. DIFFERENTIAL SCANNING CALORIMETRY (DSC)**

All DSC scans were collected using TA Instruments DSC 2920 Modulated DSC. The sample pans were high volume pans (TA Instruments). These pans can hold up to 75  $\mu\text{L}$  of material with a O-ring seal up to 250  $^{\circ}\text{C}$  as long as the vapor pressure inside does not exceed 3.8 MPa. The hair samples were saturated with water in the pans. Water saturation was achieved by placing a massed amount of hair in a vial and adding enough water to the hair to wet the hair without adding excess bulk water. No standing water was visible in these samples. From both masses (water and hair), an estimated ratio of hair and water was determined. The average composition of the mixture was roughly 37% hair and 63% water. The saturated hair was then added to a massed pan and the pan was sealed and massed again. When adding the hair and water mixture to the pan, careful

attention was made to ensure a uniform distribution of the mixture on the bottom to the pan. The average amount of hair and water mixture added to the pans was 30 mg. Other research described a method of preparing the samples by adding hair to pan and then adding water, rather than mixing the hair and water in a vial; the pan was then sealed and allowed to equilibrate for 24 hours before DSC analysis (Wortmann 2002).

In the DSC experiment, the samples were ramped 10 °C per minute from 30 °C to 250 °C using an empty pan for reference. During initial DSC trials the samples were cycled by ramping the temperature up to 250 °C then down to 30 °C, then up again to 250 °C. However, no endothermic peaks were observed during the 2<sup>nd</sup> run, meaning the hair was decomposed enough to not give any information after the 1<sup>st</sup> ramp up, so only the 1<sup>st</sup> temperature ramping was used for analysis. An important aspect during the sample preparation was to not exceed the pan pressure and sample mass limits. Not doing this could cause the pan to rupture and contaminate the DSC cell.

### **3.2. THERMOGRAVIMETRIC ANALYSIS (TGA)**

The TGA measurements were performed using TA Instruments Hi-Res 2950 TGA Thermogravimetric analyzer. Initial samples were ramped 20 °C per minute to 900 °C. The amount of hair used for each analysis varied from 0.6-3.1 mg, but no difference in mass loss steps was observed based on amount of sample used. The length of the chopped hair also did not appear to affect the mass loss results. Variation of the mass loss for the different samples was observed from 450-550 °C presumably due to treatments, so reproducing the analysis was necessary. However, because of the small sample sizes, additional samples (lot 2) were obtained for reproducibility analysis. The samples obtained included untreated as well as two treated samples which were the same as two treatments from the original set of samples (lot 1). Further analysis with the samples from lot 2 showed that the optimum experiments were ramped 5 °C per minute to 750 °C. When heating the samples at 20 °C per minute, the line shapes were similar but not the same. Decreasing the heating rate to 5 °C per minute gave reproducible results. The slower heating rate shifted the mass loss steps to lower temperatures but the thermograms retained the same general shape.

### 3.3. FOURIER TRANSFORM INFRARED SPECTROSCOPY (FTIR)

The instrument used for the IR experiments was a Nicolet Nexus 470 FTIR. Data was collected for the spectra from 600 to 4000  $\text{cm}^{-1}$  with 1024 scans. KBr pellets were made by mixing hair and KBr (Aldrich) at an approximate ratio of 1:100 hair to KBr. The mixture was ground vigorously in order to make the hair pieces smaller and ensure uniform distribution. Exposure to the atmosphere was avoided as much as possible to prevent water absorbing to the pellet.

### 3.4. $^{13}\text{C}$ CROSS POLARIZATION/MAGIC ANGLE SPIN (CP/MAS) NMR

The  $^{13}\text{C}$  CP/MAS NMR spectra were obtained using an Oxford 400 MHz magnet with a Tecmag Discovery console and NTNMR software which operated on a Windows system. The CP/MAS probes used were made by Doty Scientific. Initial analysis was done using a probe with a 7 mm sample size. The 7 mm standard sample containers consist of zirconia rotors with Kel-F caps, and have the capability to hold 200-350  $\mu\text{l}$  of material and spin up to 6 kHz. The hair samples were added to the sample containers, although the sample size was too small to completely fill the container, so proper packing was not possible. Experiments using this probe included standard  $^{13}\text{C}$  CP/MAS, total suppression of spinning sidebands (TOSS)  $^{13}\text{C}$  CP/MAS which removes the spinning sidebands, and dipolar dephasing (DD) TOSS  $^{13}\text{C}$  CP/MAS which decreases the intensity of protonated carbons and increases the intensity of non-protonated carbons.

The pulse sequence for a standard  $^{13}\text{C}$  CP/MAS experiment is shown in Figure 3.1. After an initial 3 second delay (d1) there was a  $90^\circ$   $^1\text{H}$  pulse (p1), followed by simultaneous  $^1\text{H}$  and  $^{13}\text{C}$  pulsing (p2 and p3), which was the cross polarization or mixing time. The data was acquired with a high power proton decoupling.

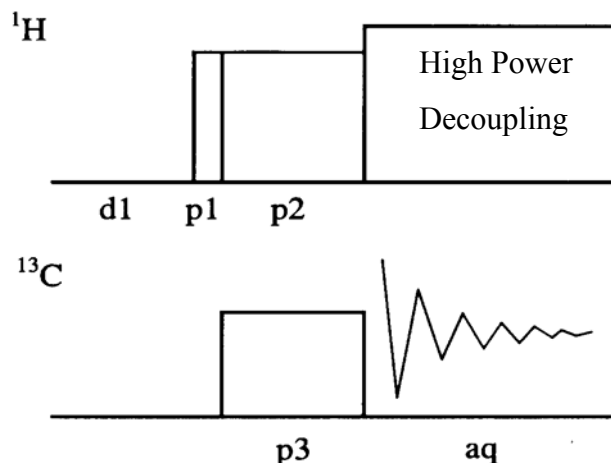


**Figure 3.1.** Pulse sequence for standard  $^{13}\text{C}$  CP/MAS NMR experiment. From: Braun, S., Kalinowski, H.-O., Berger S., *150 and More Basic NMR Experiments*, Wiley, Weinheim, Germany, 1998.

TOSS  $^{13}\text{C}$  CP/MAS experiments begin similar to a standard  $^{13}\text{C}$  CP/MAS experiment except four  $180^\circ$  pulses were applied before acquisition collection to remove spinning sidebands. Spinning sidebands are due to inhomogeneous interactions larger than the spinning frequency. The delay times ( $d2$ ,  $d3$ ,  $d4$ ,  $d5$ ,  $d6$ ) between the  $^{13}\text{C}$  pulses were calculated as a function of the spinning speed. The pulse sequence for TOSS  $^{13}\text{C}$  CP/MAS experiments is shown in Figure 3.2.

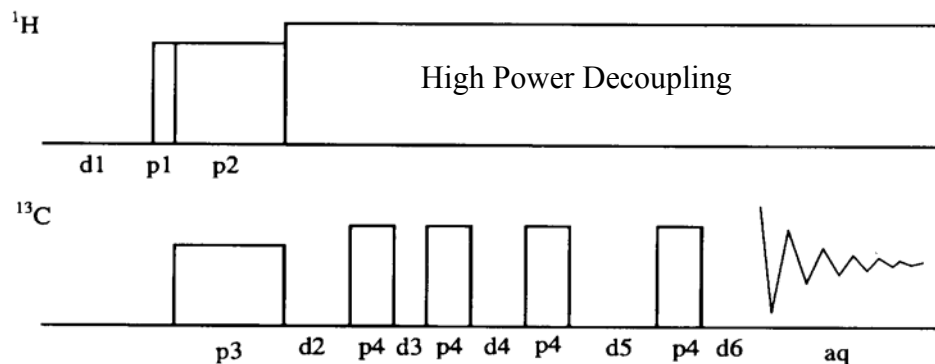


**Figure 3.2.** Pulse sequence for a TOSS  $^{13}\text{C}$  CP/MAS NMR experiment. From: Braun, S., Kalinowski, H.-O., Berger S., *150 and More Basic NMR Experiments*, Wiley, Weinheim, Germany, 1998.

DD TOSS  $^{13}\text{C}$  CP/MAS experiments were used to intensify the non-protonated carbons and decrease the intensity of protonated carbons. The experiment was done with a similar pulse sequence to a TOSS  $^{13}\text{C}$  CP/MAS experiment except the high power proton decoupling was turned off for a period of time to allow strongly coupled spins to dephase causing broadened peaks. The pulse sequence for dipolar dephasing is shown in Figure 3.3. A 60  $\mu\text{s}$  delay in the high power coupling produces a spectrum with small and broad C – H peaks and more intense non-protonated carbon peaks, such as carbonyl peaks.

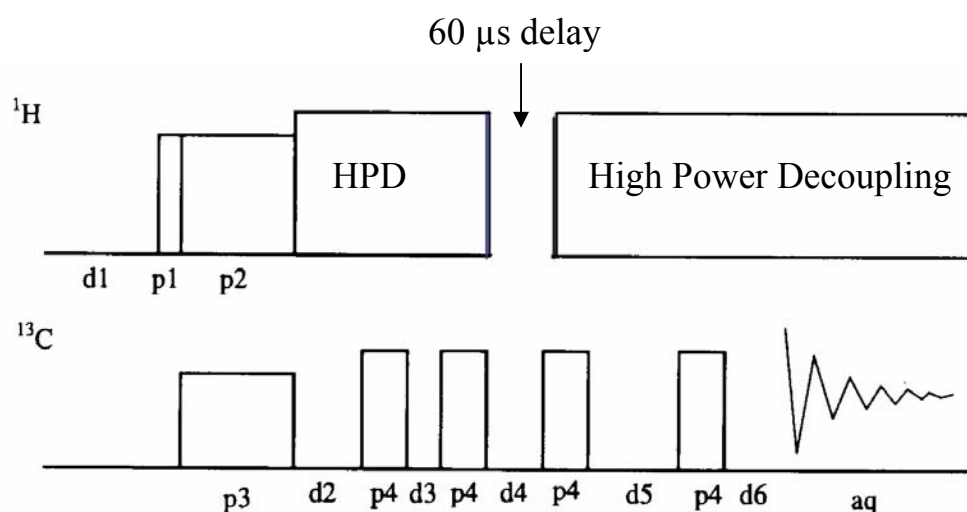


**Figure 3.3.** Pulse sequence for a DD TOSS  $^{13}\text{C}$  CP/MAS experiment. From: Braun, S., Kalinowski, H.-O., Berger S., *150 and More Basic NMR Experiments*, Wiley, Weinheim, Germany, 1998.

Once the samples were packed, they were loaded into the probe and spun at the fastest and stable speed allowable. The experiments and the spinning speeds in kHz are shown in Table 3.2.

Sample	CP/MAS	TOSS CP/MAS	DD TOSS CP/MAS
A	3.3	3.3	3.3
B	3.3	3.3	3.2
C	3.0	3.0	3.0
D	2.2	2.3	2.2
E	2.3	2.8	N/A

**Table 3.2.** The spinning speeds in kHz of each experiment using the 7 mm probe.

Further experiments were performed using a probe with a 5 mm sample size and the ability to spin faster. The sample containers were composed of silicon nitride rotors and Kel-F caps and can hold 60 – 110  $\mu$ l of material. Hair samples were packed in the sample containers and each sample filled the container except for sample B. A sandwich type packing was done for sample B, with alumina on the outside and sample B hair in the middle. Only standard  $^{13}\text{C}$  CP/MAS experiments were completed using the 5 mm probe. Table 3.3 shows the spinning speeds of each experiment with the 5 mm probe. Approximately 15,000 scans were obtained for all experiments from both probes. Although the spinning speeds were initially stable at the speed reported, the time required to collect data (up to 20 hours) usually caused the spinning speed to decrease up to 500 Hz.

Sample	CP/MAS
A	4.4
B	4.1
C	3.8
D	4.8
E	4.2

**Table 3.3.** The spinning speeds in kHz of each experiment using the 5 mm probe.

The effect of high temperature on hair was also analyzed. Hair from a donor (Dr. Tadashi Tokuhira) was exposed to 350 °C in an oven for 16 minutes. The hair was then stored at room temperature and relative humidity of approximately 35% before a standard  $^{13}\text{C}$  CP/MAS experiment spun at 3.3 kHz.

## 4. RESULTS

### 4.1. DIFFERENTIAL SCANNING CALORIMETRY (DSC)

Figure 4.1 shows the DSC results for the untreated Caucasian hair and water. The top curve is the hair and water mixture. This curve shows an initial endotherm from 50-130 °C due to water loss from the hair fiber (Milczarek et al. 1992; Monteiro et al., 2005). At 155 °C there is a large endothermic peak presumably due to denaturing of cortical cells, and around 200 °C a broad endothermic peak is observed most likely due to the denature of keratin (Wortmann et al., 1998; Monteiro et al., 2005). The bottom curve is for distilled water. Although this line should be smooth, there are some small peaks. These peaks are from noise which could be due to a number of things such as contamination of the DSC cell or electrical noise.

### 4.2. THERMOGRAVIMETRIC ANALYSIS (TGA)

TGA analysis of hair was initially done using a 20 °C per minute ramp speed. Figure 4.2 shows the results of samples A-E ramped at this speed. The bottom-most curve is the untreated sample (A) and the top four curves are treated samples, each labeled on the right. The curves are shifted vertically to observe differences easier. The approximate sample size was 1.25 mg. The initial mass loss step from 25-130 °C is due to the loss of loosely and tightly bound water. The next step is related to the denaturing of hair keratin and organic degradation up to 400 °C. Finally, from 400-550 °C there is complete degradation of the hair keratin. A variation in mass loss from 500-600 °C was observed with the treated samples in comparison to the untreated sample, indicating that the treatments changed the structure of the hair.

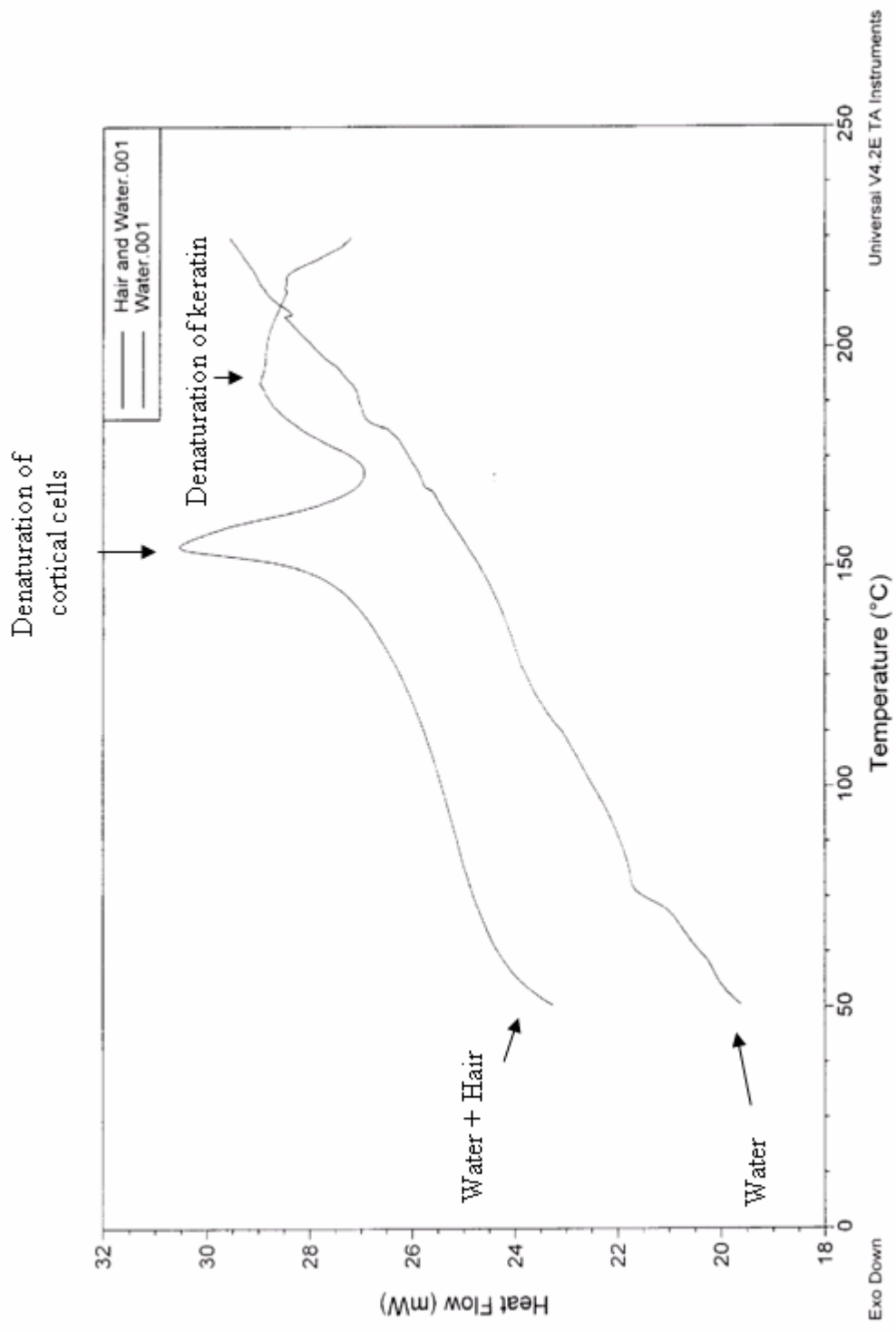


**Figure 4.1.1.** DSC curves for untreated hair with water (top curve) and water alone (bottom curve).

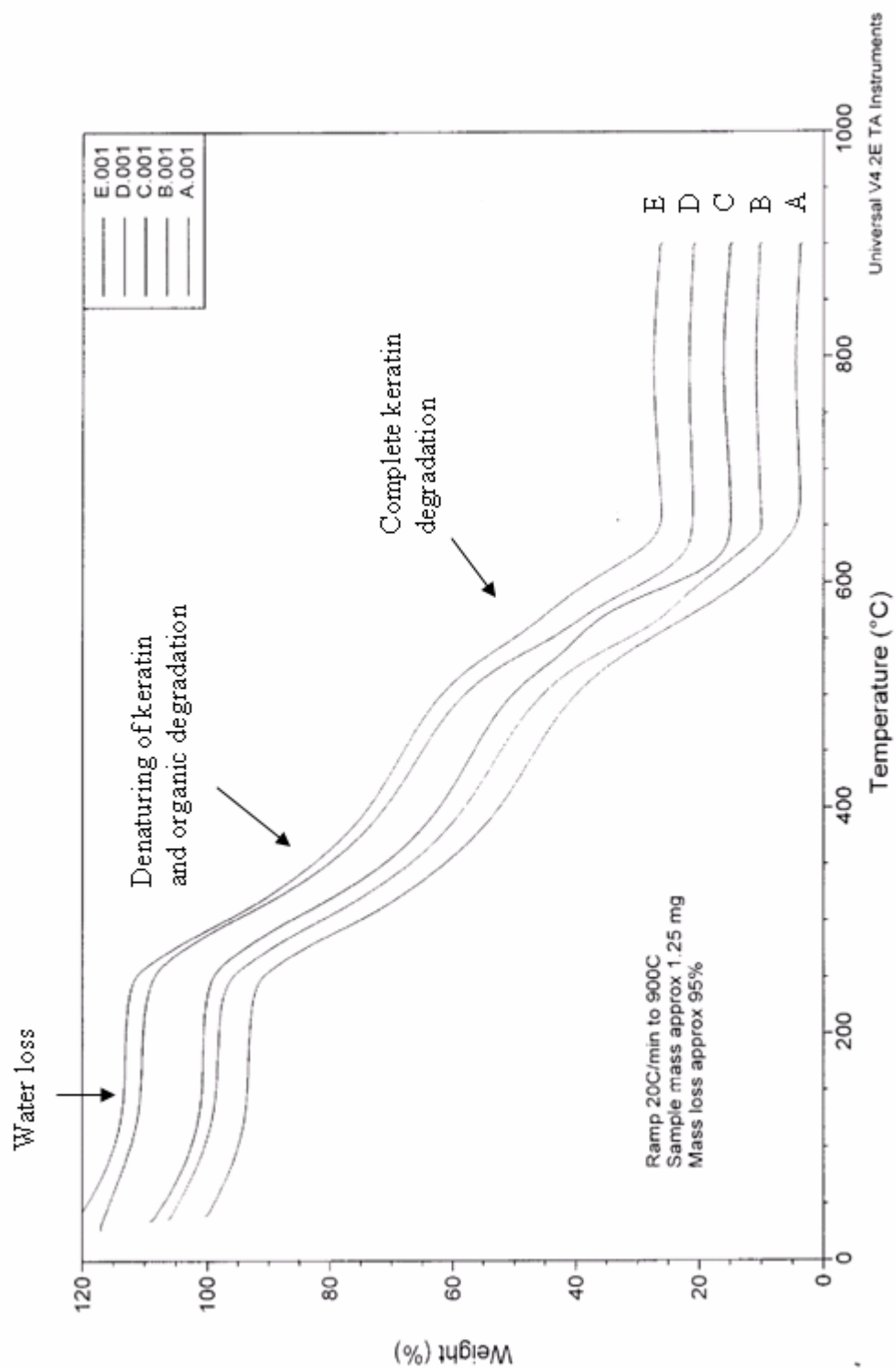
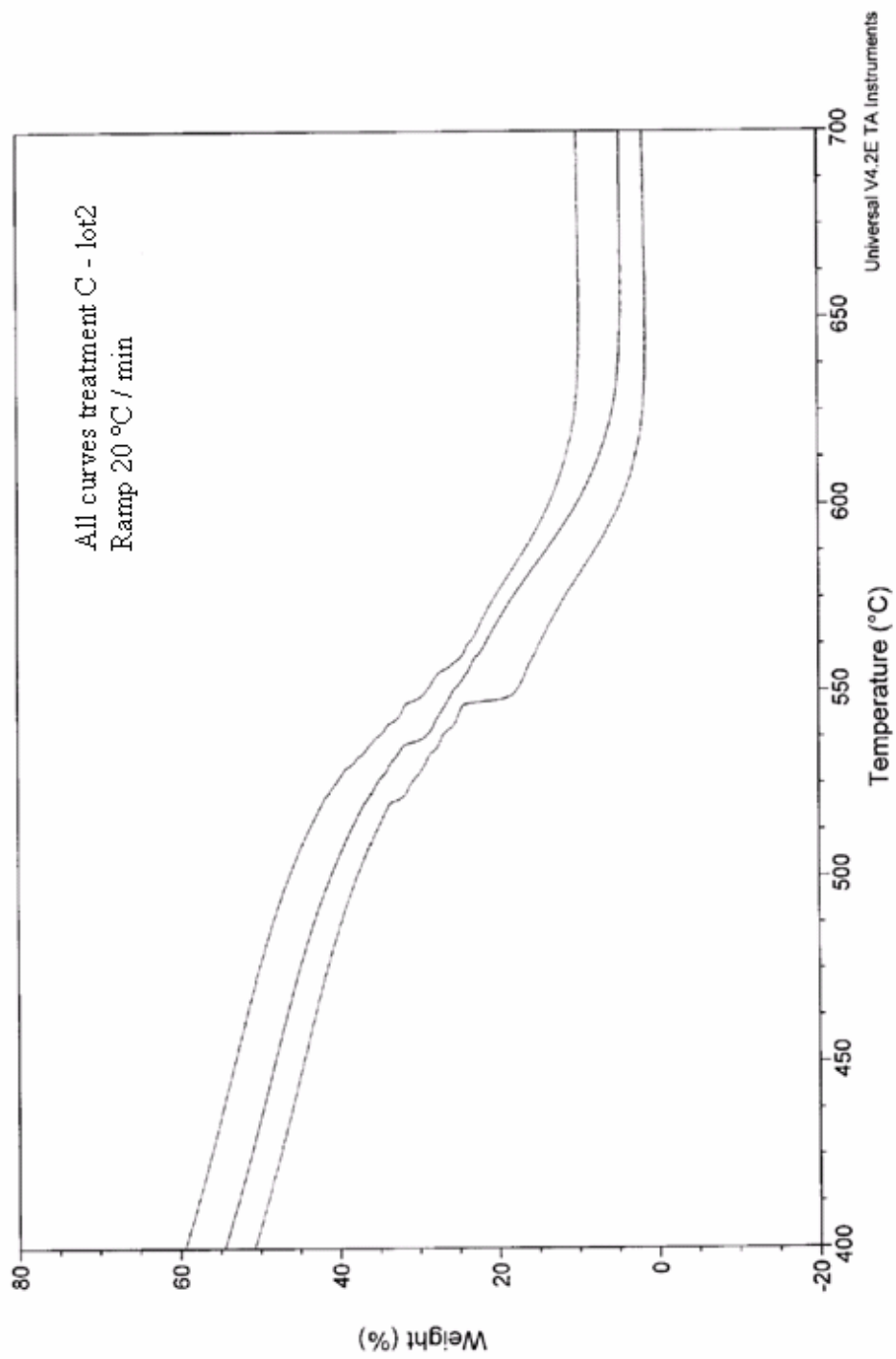


Figure 4.2. TGA curves for hair samples A – E, labeled on left.

To determine the reproducibility of the TGA experiments, more hair was obtained to run additional experiments. The additional samples included treatments A-C in larger quantities and were referred to as lot 2 because the samples came from a different subject than the initial samples (lot 1). It was determined that heating the samples at a slower heating rate of 5 °C per minute produced reproducible results, where as heating the samples at 20 °C per minute did not produce the same thermogram shape every time. Figure 4.3 shows three separate thermograms of treatment C from lot 2 heated at a rate of 20 °C per minute and zoomed into 450-650 °C region. The thermograms have a similar rough shape over that temperature interval, but they are not similar enough to be reproducible. When heated at a slower rate of 5 °C per minute the thermograms are much more reproducible. Figure 4.4 shows two thermograms each for treatments B and C from lot 2 compared to an untreated sample, all heated at 5 °C per minute. The curves for each treatment are reproducible.

The samples from lot 1 were analyzed again at a heating rate of 5 °C per minute, as shown in Figure 4.5. When comparing Figure 4.5 (5 °C per minute) to Figure 4.2 (20 °C per minute), the shapes from corresponding treatments are very similar and there is still an observable difference in mass loss between the untreated sample and the treated samples, which further confirms that the treatments are changing the structure of the hair. The treated hair samples lose mass slower than the untreated hair samples. Treatment C loses mass the slowest, followed by treatments B and E, while treatment D retains a very similar shape to the untreated sample (A) but has a slightly rough shape.



**Figure 4.3.** TGA curves for hair sample C from lot 2 showing that curves are not reproducible at a faster heating rate of 20 °C per minute.

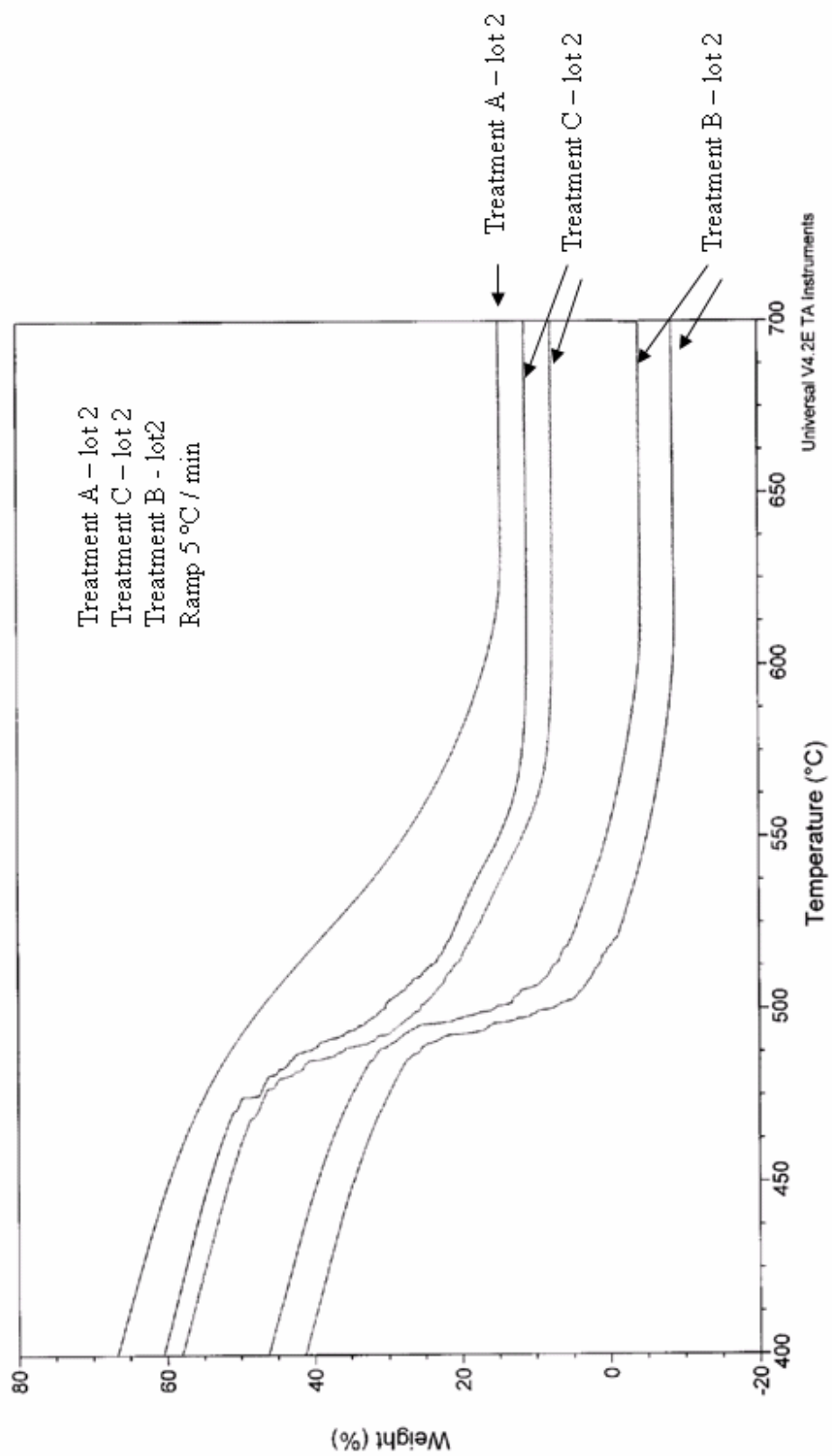


**Figure 4.4.** TGA curves for hair samples A - C from lot 2 showing that curves are reproducible at a slower heating rate of 5 °C per minute.

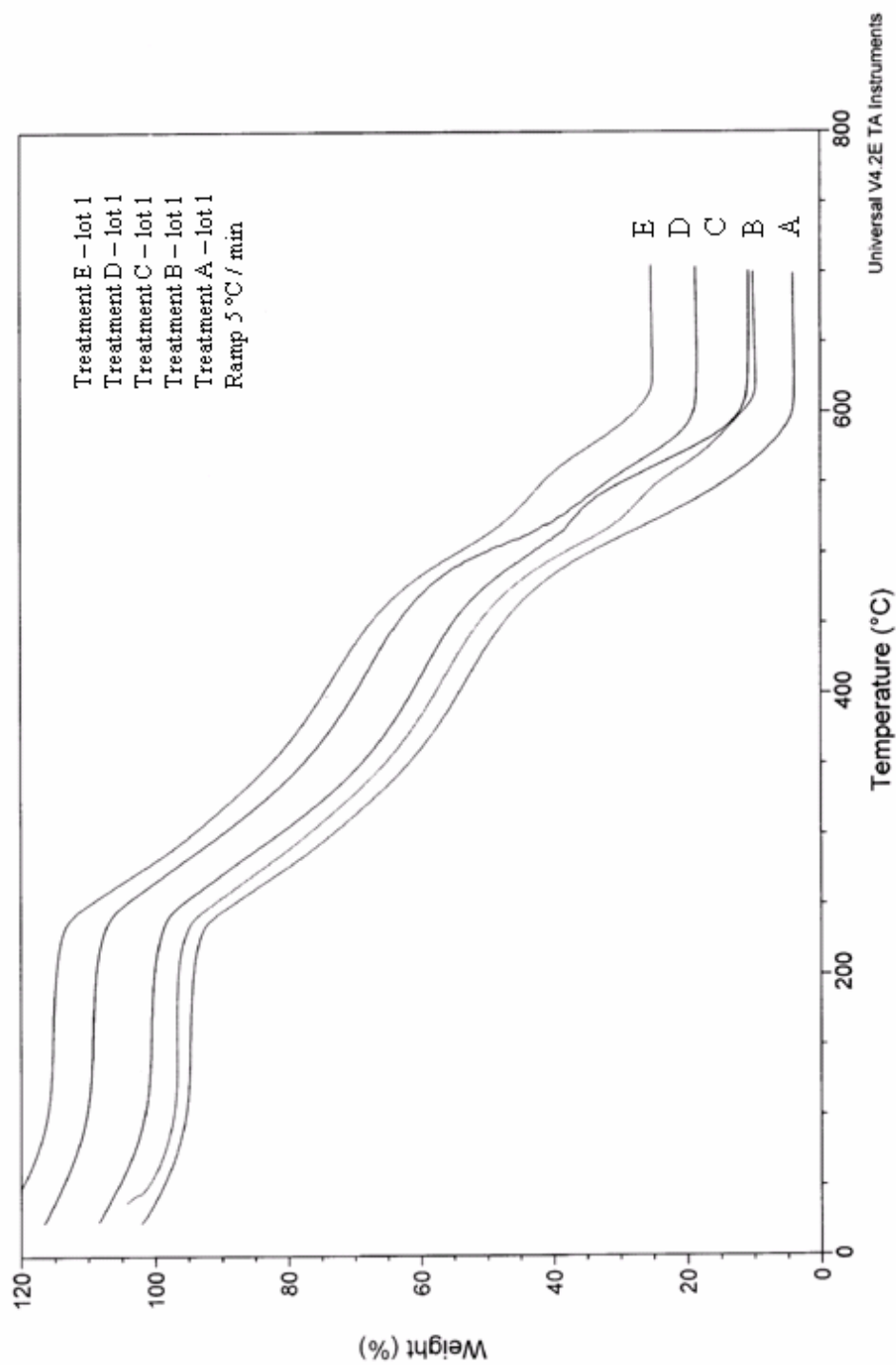


**Figure 4.5.** TGA curves for hair samples A - E from lot 1 heated at a rate of 5 °C per minute.

Samples heated at a lower heating rate of 5 °C per minute had curves similar to those at higher rates, (20 °C per minute), but the mass loss temperatures were shifted to lower temperatures. Figure 4.6 shows this by comparing treatment A from lot 2 heated at the two different heating rates of 5 °C per minute (bottom curve) and 20 °C per minute (top curve).

To verify that the length of hair samples did not affect the TGA results, hair from a donor (Dr. Tadashi Tokuhira) was obtained and samples of three different lengths were cut. The lengths were approximately 1 mm (short), 3 mm (medium), and 5 mm (long). Figure 4.7 shows the curves of the three samples which were heated at a rate of 20 °C per minute. The curves are separated vertically for better comparison. No difference in curve shape was observed between the three samples, suggesting that the length of the hair samples does not change the mass loss steps.

Another observation noticed when using the TGA is that the same treatment causes different changes to different samples. For example, Figure 4.8 compares treatment B's effect on hair from lot 1 and 2, which are from different individuals. The top curve is treatment B from lot 1 and the bottom curve is treatment B from lot 2. The middle two curves are both untreated, top is from lot 1 and the bottom is lot 2. All samples were heated at a rate of 5 °C per minute. The untreated samples looked very similar to each other, but the treatment B hair samples were very different. Treatment B from lot 2 lost mass faster and had a rough shape compared to treatment B from lot 1, which lost mass slower than the untreated samples and had a smooth line shape. Although the treatments may be the same, the effect that they have on different individual's hair may vary.

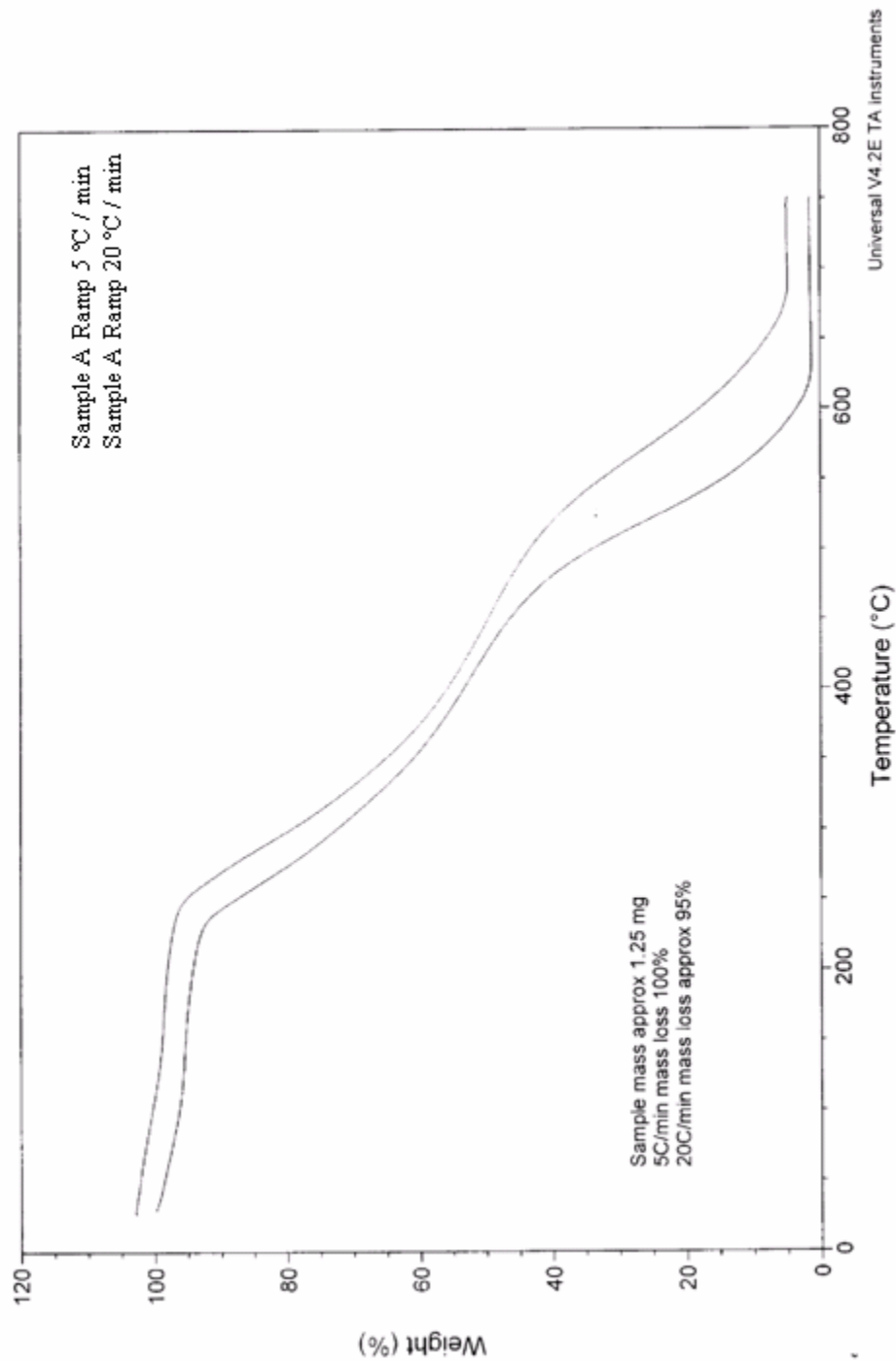


**Figure 4.6.** TGA curves for hair sample A from lot 2 heated at a rate of 5 °C per minute (bottom curve) and 20 °C per minute (top curve).

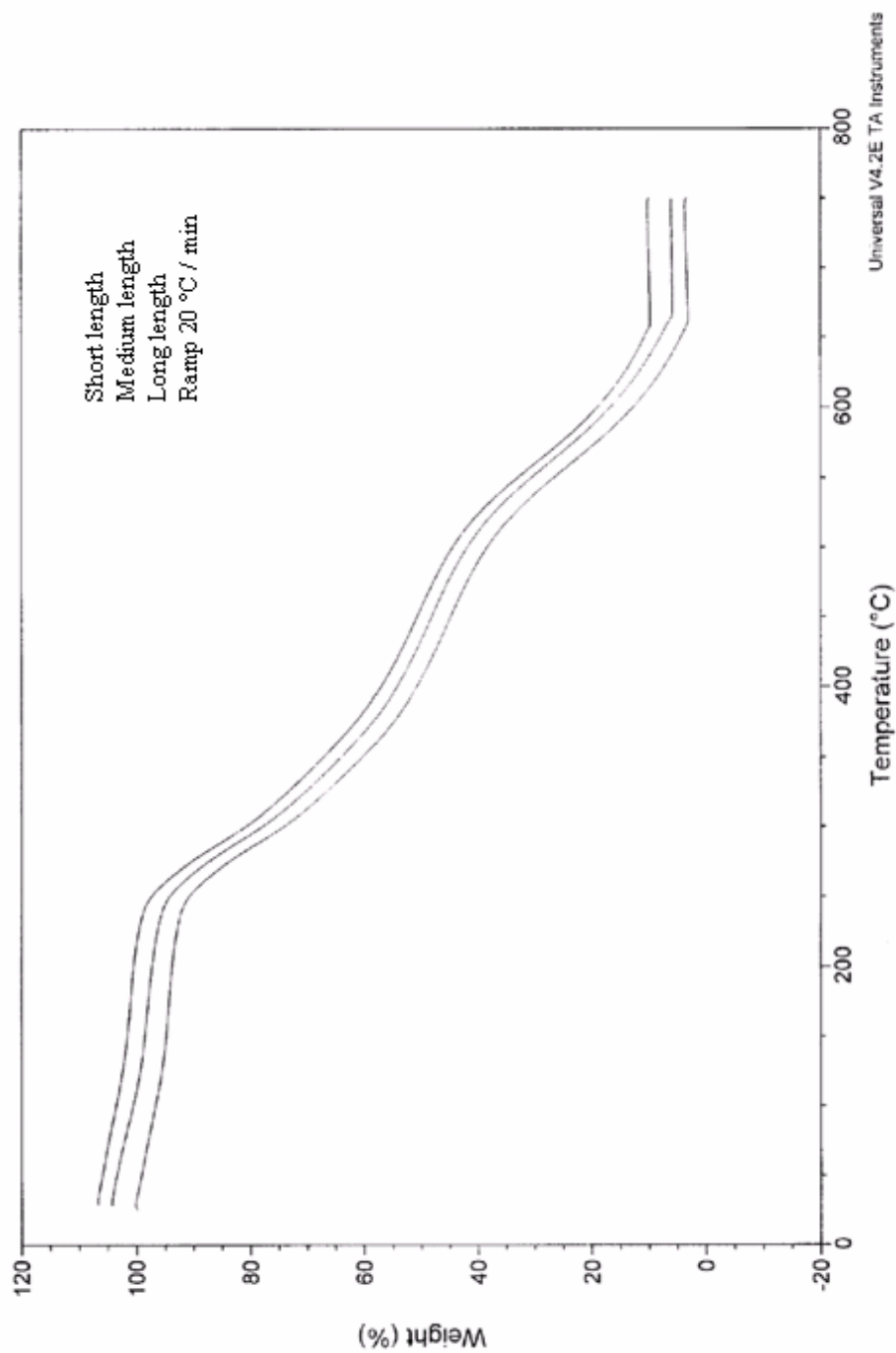


**Figure 4.7.** TGA curves for hair sample from donor. The hair samples were chopped to different lengths to show that length of the hair fiber does not effect the results. Top curve is short length, middle curve is medium length, and bottom curve is long length.

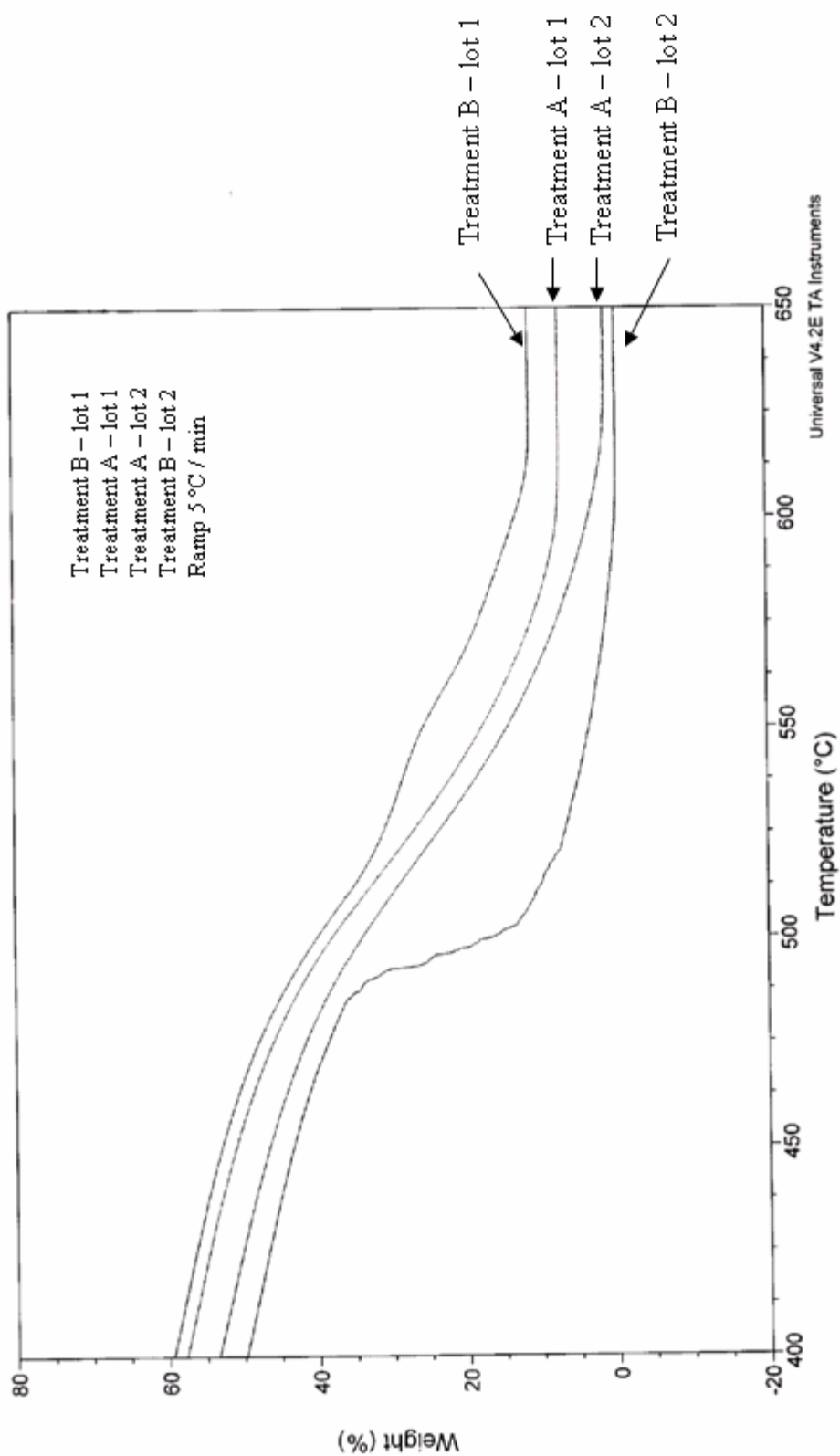


**Figure 4.8.** Comparison of treatment B's affect on hair from lot 1 and 2. The two outer curves are treatment B and the two middle curves are treatment A (untreated).

### 4.3. FOURIER TRANSFORM INFRARED SPECTROSCOPY (FTIR)

FTIR was used to determine the structural changes to hair when exposed to various treatments. FTIR penetrates the outer surface of the hair which is the cuticle. The cuticle is primarily composed of cystine, along with other amino acids which are not usually found in alpha helical polypeptides. The hair treatments that were analyzed are reducing and oxidizing treatments which break the disulfide bond in cystine and convert it to cysteic acid, cystine monoxide (R-SOS-R), and cystine dioxide (R-SO<sub>2</sub>S-R).

A rough comparison of the spectra showed that all hair samples were very similar. The spectra of the samples are shown in Figure 4.9. The spectra have been normalized and separated vertically to see the differences more easily. Each spectrum has been labeled on the left side according to the treatment type. All samples, including the untreated one, showed oxidation based on the peaks exhibited. Most likely this oxidation is due to environmental factors such as ozone causing oxidation of the hair surface. A summary of the peaks found in the spectra is given, along with peak assignments in Table 4.1.

It is important to note that most samples showed a peak at each of the listed frequencies; however, the overall intensity did vary among the samples. There were some small differences such as the 1040 cm<sup>-1</sup> peak, which were weak in samples C and D and fairly strong for E, and a primary amine peak at 3315 cm<sup>-1</sup>, shown only in samples C, D, and E spectra. Samples A and B showed relatively weak intensities for all peaks when compared to samples C, D, and E. The difference in intensities is possibly due to sample preparation. KBr pellets were made with hair to ensure that a hair fiber would be in the path of the IR beam, more hair may have been added to some of the samples.

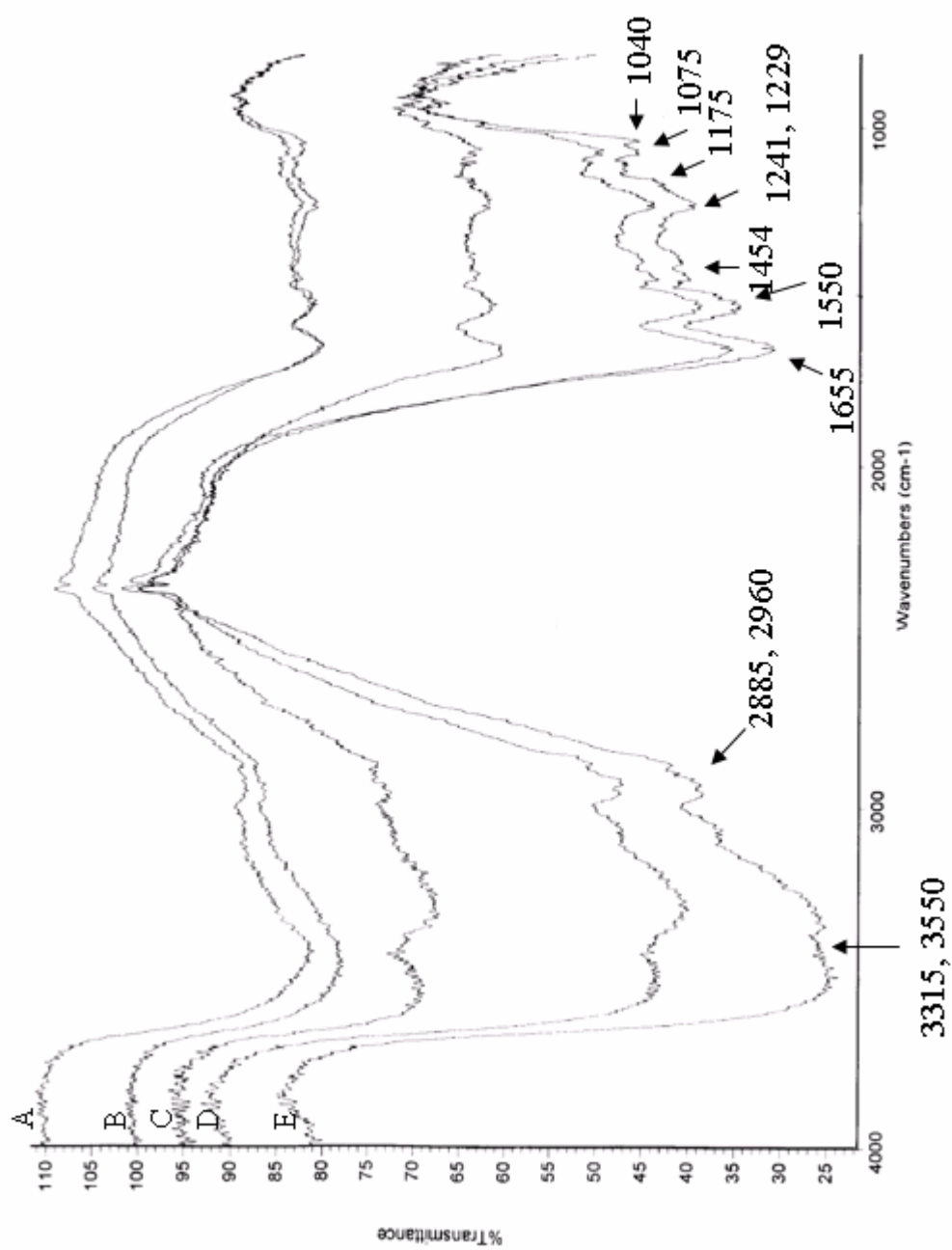


Figure 4.9. FTIR spectra of sample A – E from lot 1, labeled on left.

The quality of the spectra obtained was comparable to other studies of hair using IR, especially considering the method of sample preparation. FTIR may not be the best method to determine changes in hair structure. IR radiation does not penetrate hair and so a lot of reflectance may occur when using hair fibers. Also, determining amount of oxidation from the treatments is difficult since hair naturally gets oxidized from environmental factors.

IR resonances at 1040, 1075, 1175, and 1229  $\text{cm}^{-1}$  all correspond to different products of cystine oxidation. The other peaks at 1241, 1454, 1550, and 1655  $\text{cm}^{-1}$  are related to typical amino acids.

Wavenumbers ( $\text{cm}^{-1}$ )	Assignment
1040	sulfonate, S-O sym. stretch
1075	cystine monoxide (R-SO-S-R)
1175	sulfonate, S-O asym. stretch
1229	cystine dioxide (R-SO <sub>2</sub> -S-R)
1241	amide III (N-H stretch)
1454	CH <sub>2</sub>
1550	amide II (C-N stretch)
1655	amide I (C=O stretch)
2885	CH
2960	CH
3315	NH (Primary amine)
3550	OH (H <sub>2</sub> O)

**Table 4.1.** Summary of FTIR peak placements with the corresponding assignments.

#### 4.4. <sup>13</sup>C CROSS POLARIZATION/MAGIC ANGLE SPIN (CP/MAS) NMR

<sup>13</sup>C CP/MAS NMR spectra were obtained for each sample from lot 1. The first set of spectra were collected using the 7 mm probe. The experiments using this probe included standard <sup>13</sup>C CP/MAS, TOSS <sup>13</sup>C CP/MAS, and DD TOSS <sup>13</sup>C CP/MAS. Figures 4.10 - 4.14 show the standard <sup>13</sup>C CP/MAS of each treatment A-E and Figure

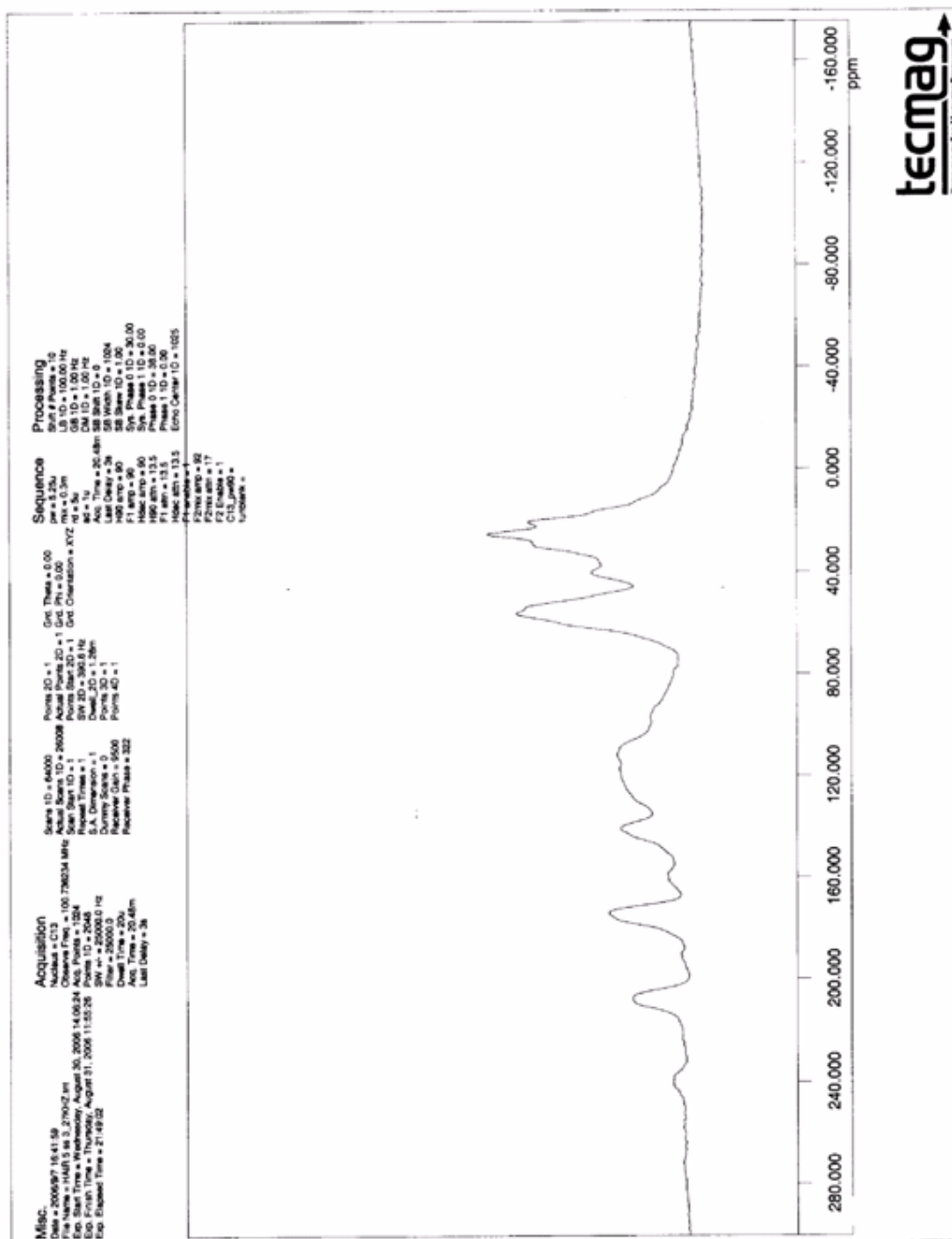
4.15 shows the spectra of all samples together for closer comparison. Spinning side bands are labeled with an asterisk in the comparison figures.

The NMR spectra show 4 basic peaks: aliphatic, C<sup>α</sup> methine, aromatic, and carbonyl. Peak assignment for <sup>13</sup>C CP/MAS NMR of hair is shown in Table 4.2 along with the amino acids which are most likely responsible for the peaks. The side chain aliphatic peak from 10-40 ppm has three smaller peaks at the top. The smaller peaks which are the most upfield are due to the least deshielded side chain aliphatic <sup>13</sup>C atoms from amino acids such as leucine and isoleucine, and the further downfield aliphatics are from amino acids with more deshielding such as lysine and arginine.

<b>Peak Placement (ppm)</b>	<b>Peak Assignment</b>	<b>Amino Acids Responsible</b>
10-40	Side chain aliphatic	Ile, Leu, Ala, Val, Pro, Lys, Arg, Thr
45-65	C <sup>α</sup> methine	Phe, Tyr, Ser, Thr, Asp, Glu, Leu, Cys
115-158	Aromatic	Phe, Tyr, Trp
172-180	Carbonyl	All amino acids

**Table 4.2.** Peak assignments for the <sup>13</sup>C CP/MAS of hair and the amino acids responsible for the peaks.

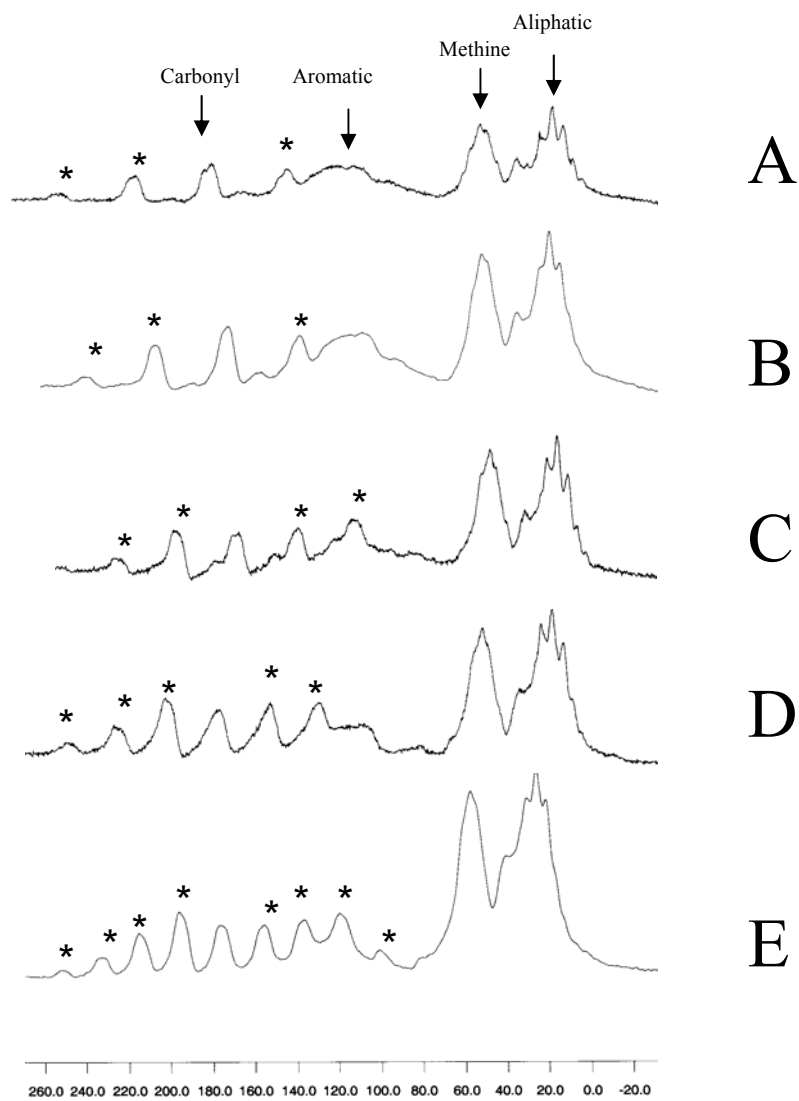


Figure 4.1.1. Standard  $^{13}\text{C}$  CP/MAS spectrum of sample B.









**Figure 4.15.**  $^{13}\text{C}$  CP/MAS NMR spectra of all samples (A – E) together for closer comparison. Spinning sidebands are denoted with an asterisk (\*).

The spectra from the standard  $^{13}\text{C}$  CP/MAS showed some variations among the different samples. First, the peak shape for the aliphatic, methane, and carbonyl peaks are slightly different for each sample, however, samples C and D are very similar to each other. Unfortunately, the aromatic resonances overlap with a spinning side band for samples C, D, and E, so any differences are hard to discern. Previous research (Nishikawa, N. et al. 1998 – a) has observed damage caused by permanent waving by comparing the peak shape of the carbonyl peak. Although the peak shapes are slightly different for each sample in this case, the differences could be due to variations during processing the spectra such as phasing, or the quality of the spectrum collected.

Since spinning side bands were a problem in the standard  $^{13}\text{C}$  CP/MAS, TOSS experiments were performed. The TOSS  $^{13}\text{C}$  CP/MAS spectra from the 7 mm probe are individually shown for samples A-E in Figures 4.16 – 4.20 as well as together in Figure 4.21 for closer comparison. Again the peak shapes are different from each other, with the aliphatic peak changing the most. The carbonyl peak is almost nonexistent in samples D and E, possibly due to inconsistent spinning speed during data collection. The aromatic peak is small and narrow in samples A and B compared to the aromatic peak in the standard  $^{13}\text{C}$  CP/MAS and could actually be a spinning sideband, while in samples C, D, and E, the aromatic peak is not observable. Due to the fact that spinning speed variations took place during data collection, the peak shapes may not be reliable enough to base conclusions of treatment effects on hair samples.











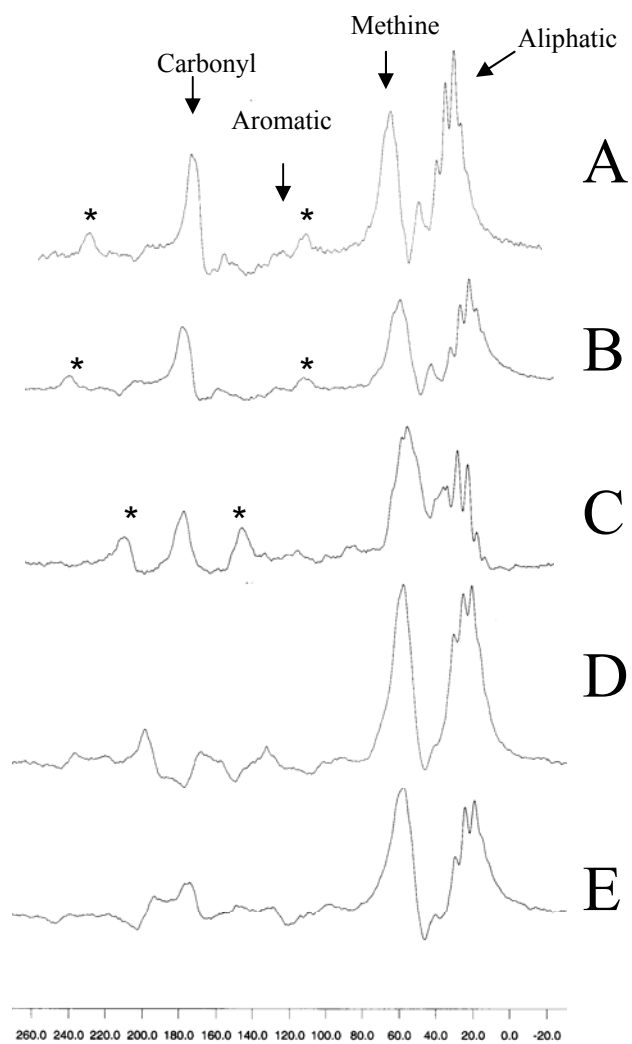


**Figure 4.21.** TOSS  $^{13}\text{C}$  CP/MAS NMR spectra of all samples (A – E) together for closer comparison. Spinning sidebands are denoted with an asterisk (\*).

For additional analysis, DD TOSS  $^{13}\text{C}$  CP/MAS experiments were performed to intensify the carbonyl peak and decrease the protonated carbon signals. Spectra of samples A-D for DD TOSS  $^{13}\text{C}$  CP/MAS experiments using the 7 mm probe are shown separately in Figures 4.22 – 4.25 and together in Figure 4.26. Data for sample E was not collected. Spectra for samples C and D show a failed experiment, again probably due to spinning speed variation, so no useful information can be obtained. Sample A showed an increase in carbonyl intensity, but the aliphatic and methine peaks were also intense and connect into one broad peak. Sample B showed an increased carbonyl peak with a decreased aliphatic and methine intensity, as the experiment is supposed to. The aromatic peak in all experiments was not observed.

A comparison of the three types of experiments, standard  $^{13}\text{C}$  CP/MAS, TOSS  $^{13}\text{C}$  CP/MAS, and DD TOSS  $^{13}\text{C}$  CP/MAS, is shown in Figure 4.27. The spectra of sample B is used to illustrate the differences of the three experiments. The top spectrum is standard  $^{13}\text{C}$  CP/MAS showing spinning side bands on the carbonyl peak. The middle spectrum is a TOSS  $^{13}\text{C}$  CP/MAS experiment where the spinning sidebands have been suppressed. The bottom spectrum is the DD TOSS  $^{13}\text{C}$  CP/MAS experiment showing an intensified carbonyl peak and a decrease in the protonated carbon peaks of aliphatic, methine, and aromatic.

Another probe which had a 5 mm sample rotor was used to obtain standard  $^{13}\text{C}$  CP/MAS spectra of the hair samples. This probe allowed for faster spinning speeds which generally gives narrower lines and fewer spinning sidebands. Figures 4.28 – 4.32 show each of the samples (A – E) individually, and Figure 4.33 displays them together.





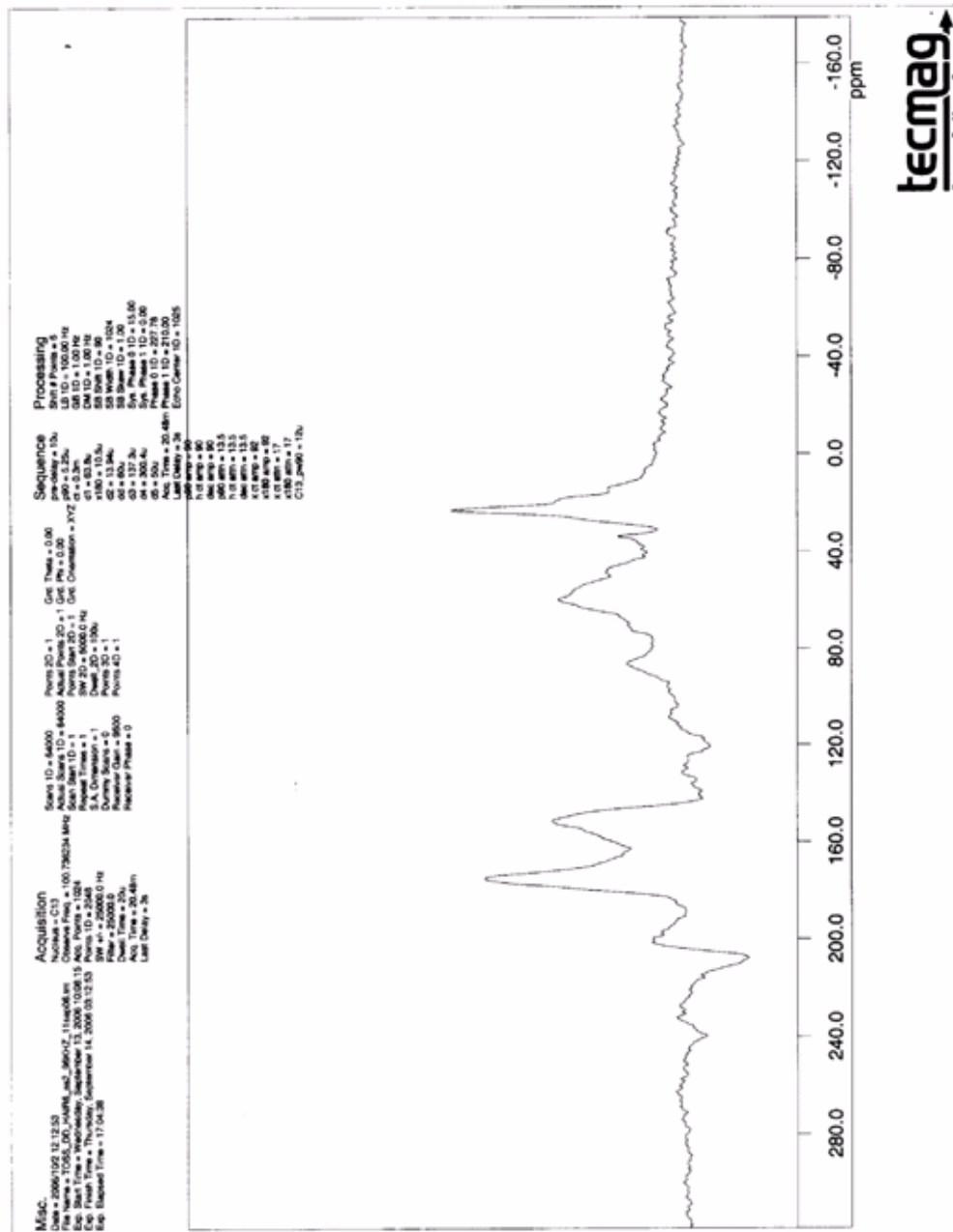
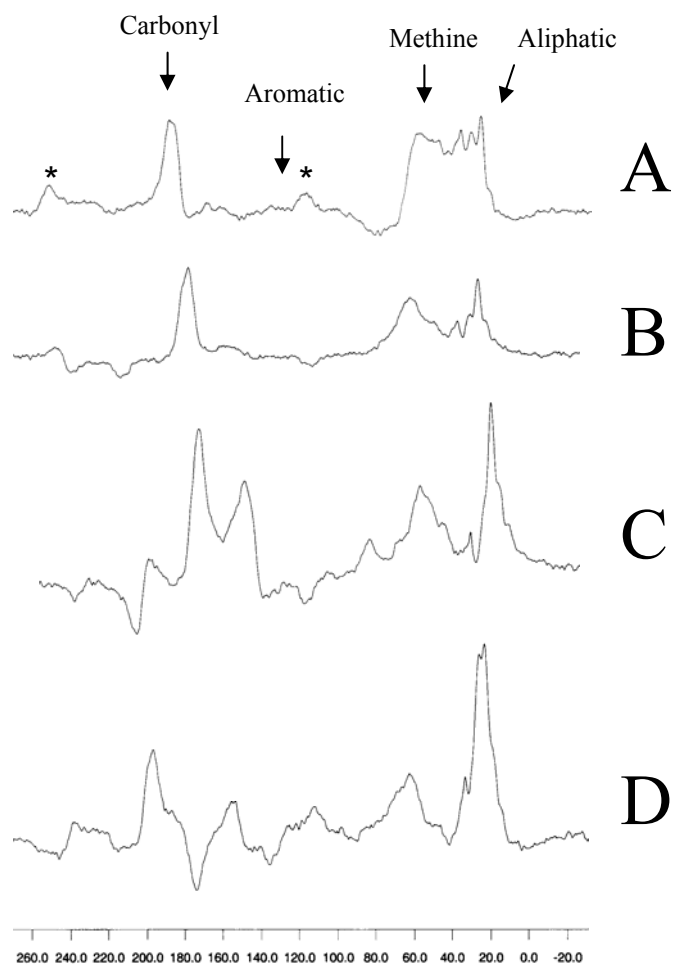
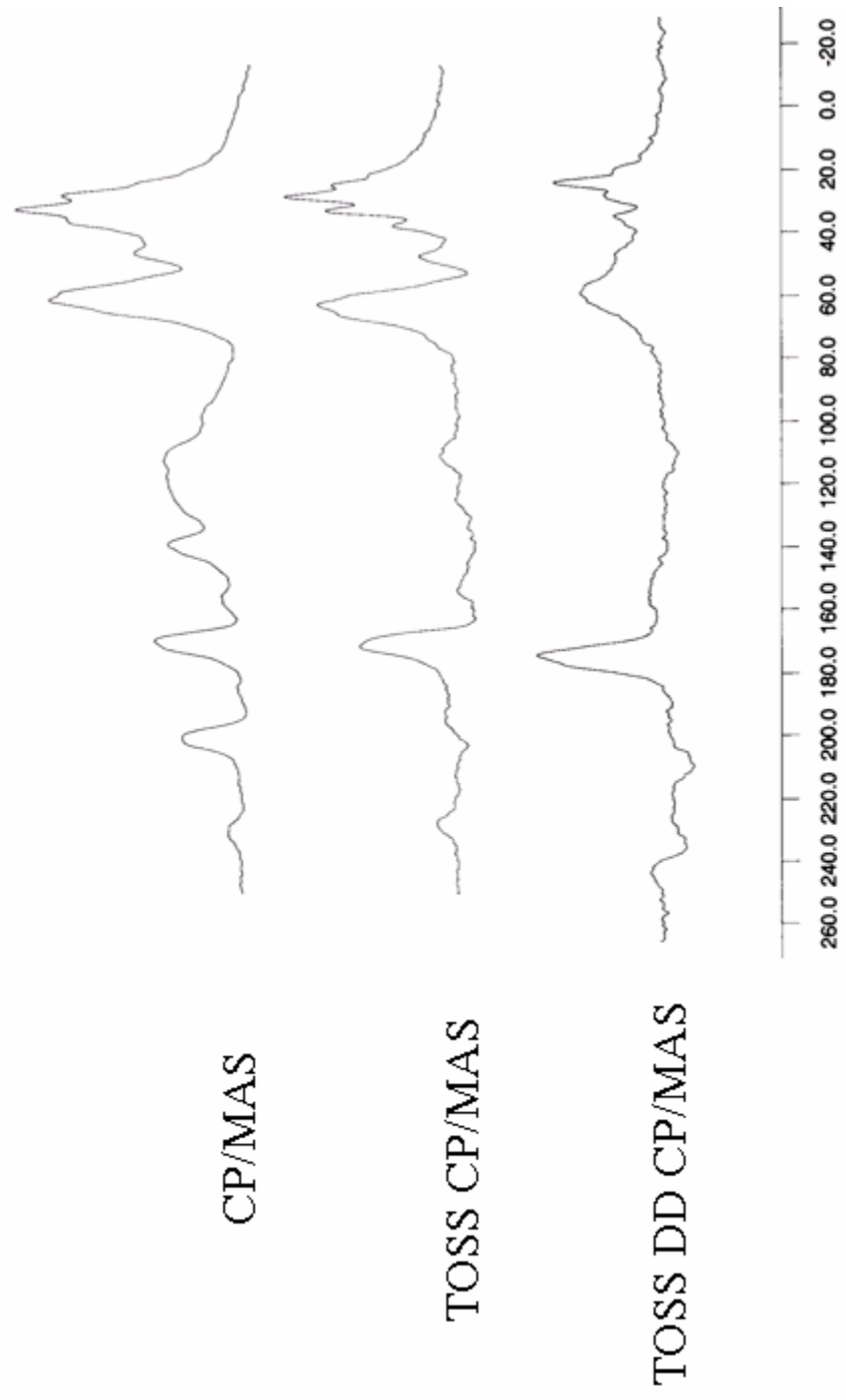


Figure 4.24. DD TOSS <sup>13</sup>C CP/MAS spectrum of sample C.





**Figure 4.26.** DD TOSS <sup>13</sup>C CP/MAS NMR spectra of samples A – D together for closer comparison. Spectrum for sample E was not obtained. Spinning sidebands are denoted with an asterisk (\*).



**Figure 4.27.** Comparison of CP/MAS experiments using sample B.

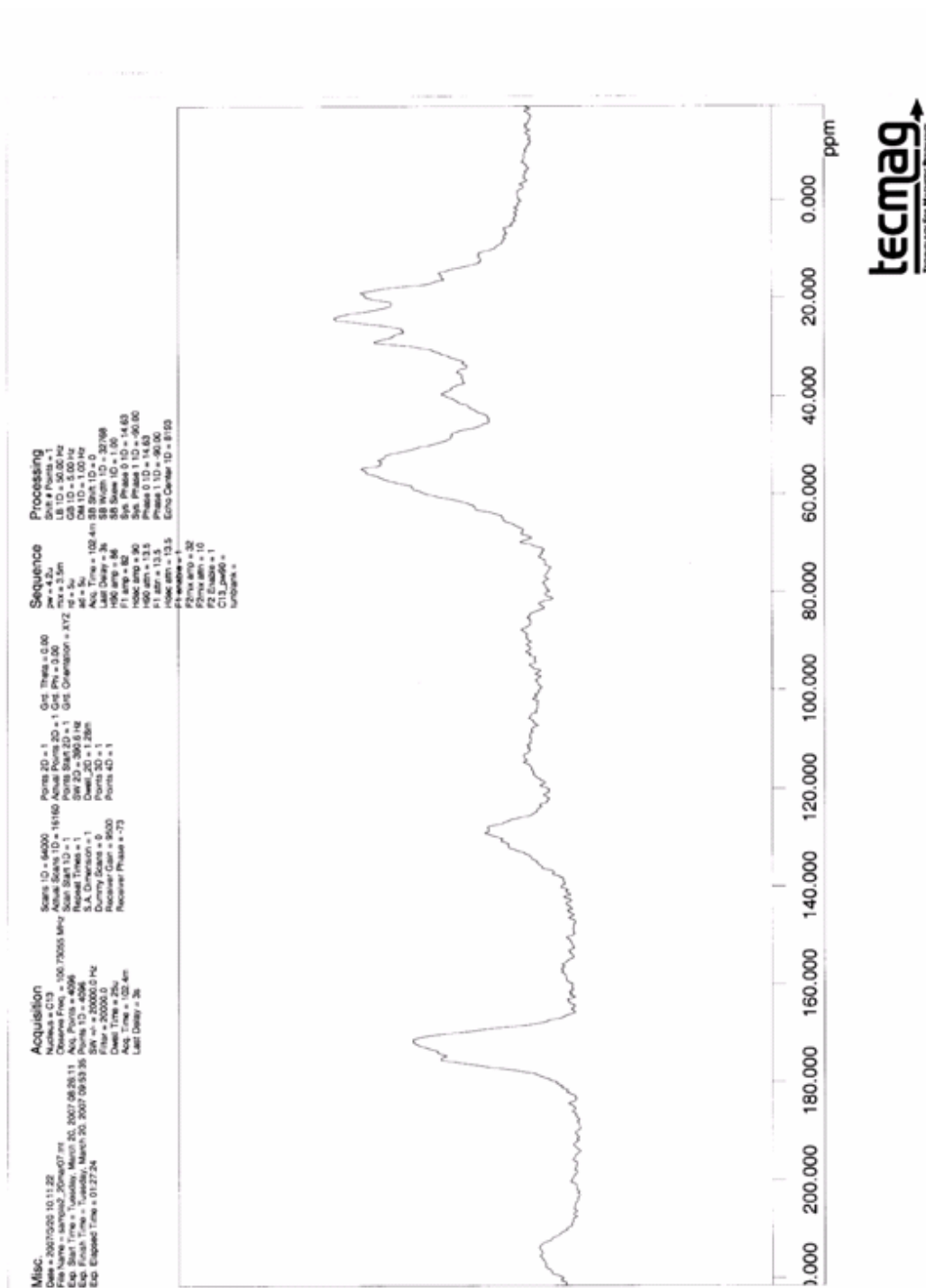


Figure 4.28. Standard  $^{13}\text{C}$  CP/MAS spectrum of sample A with 5 mm probe.



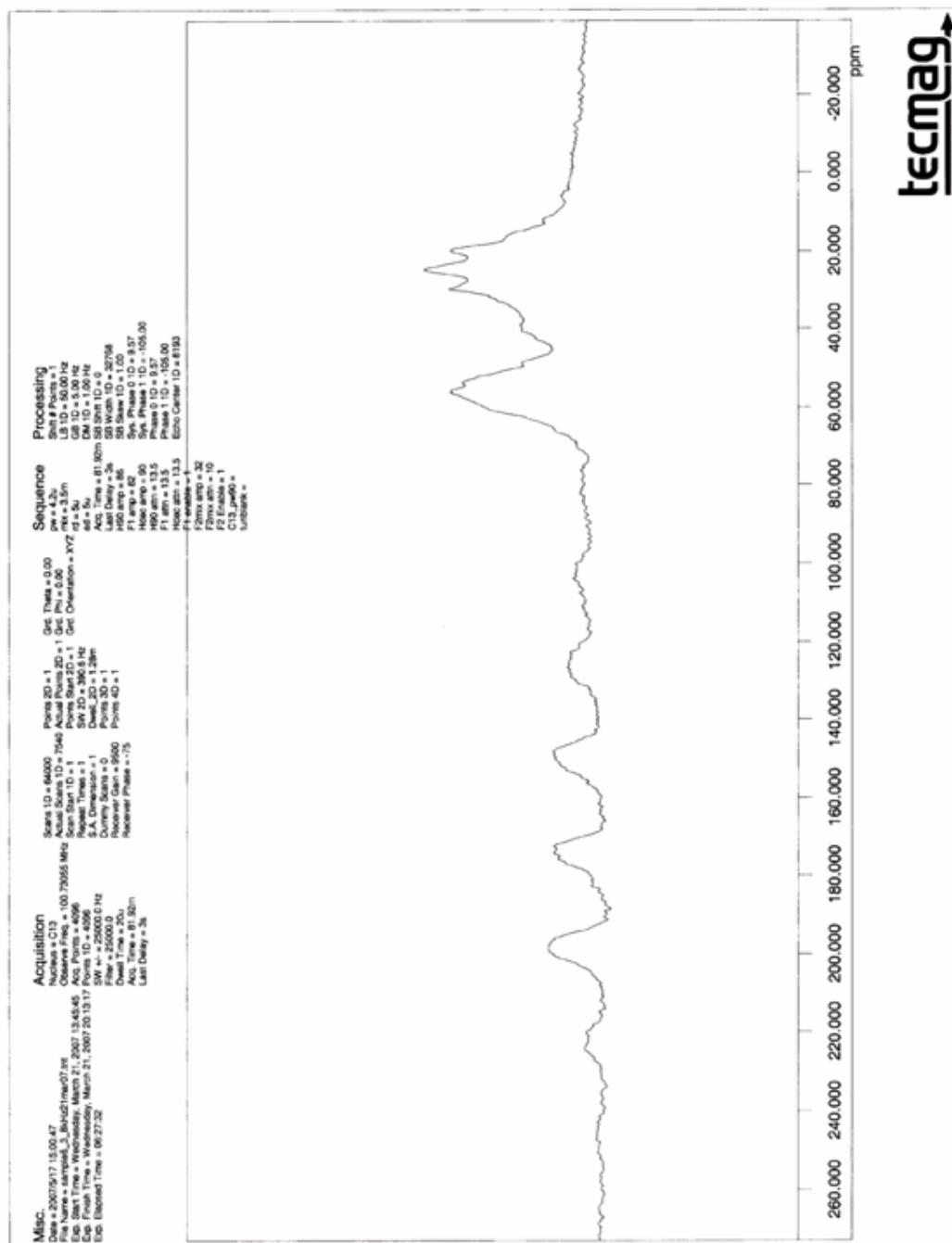
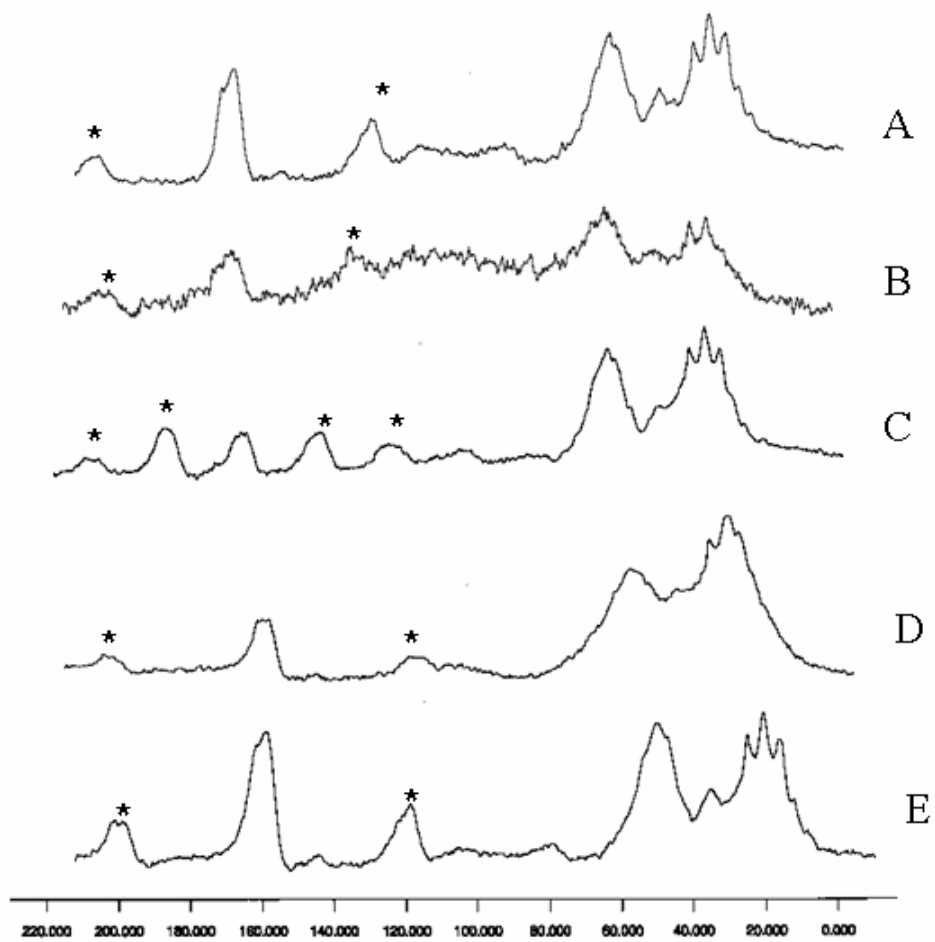


Figure 4.30. Standard  $^{13}\text{C}$  CP/MAS spectrum of sample C with 5 mm probe.







**Figure 4.33.** Comparison of standard  $^{13}\text{C}$  CP/MAS spectra of samples A - E with 5 mm probe.

The spectrum collected for sample B has poor S/N and peak intensity because the sample size was extremely small and alumina was used as filler in the sample container, so useful information is not obtainable. Samples A and E both exhibited a carbonyl peak which is equivalent in intensity as the aliphatic and methine carbon peaks. The carbonyl peak in samples C and D is small compared to the aliphatic and methine peaks. This trait was not observed from the data collected from the 7 mm probe, where the carbonyl peak was smaller for all the samples compared to the aliphatic and methine peaks. The carbonyl peak for A and E both have a top which points to the right, and samples C and D show a flat topped carbonyl peak.

The peak shape is also more consistent among the samples compared to the data from the 7 mm probe. A comparison of data from 1 experiment each, samples A, C and E, had a consistently shaped aliphatic peak which had a triple peak at the top and small humps on the side, including a smaller peak downfield at 35 ppm. The methine peak for samples A, C, and E are also very similar to each other. The aliphatic peak is small and broad in samples A, C, D, and E, and is large and broad in sample B. The spectrum of B is of poor quality because the sample size was much smaller than the other samples, and alumina was used as filler so the signal from the sample was small. It is also notable that the aliphatic and methine peak are broader and connected for sample D.

An overall comparison showed that samples A and E produced the most similar spectra, with C also comparable. The peak shape of the aliphatic and methine peaks was different from the others in that they were broader and had different shapes. The smaller carbonyl peaks and different shaped tops of samples C and D could be due to the treatments. There are also fewer spinning sidebands in the data from the 5 mm probe compared to the data from the 7 mm probe for a standard  $^{13}\text{C}$  CP/MAS. From the 5 mm probe data, sample D has the fewest and smallest spinning sidebands and sample C has the most spinning sidebands. This observation can be explained by the spinning speed. Sample D was spinning the fastest at 4.8 kHz, and sample C was spinning the slowest at 3.8 kHz.

Additional analysis was done with the 5 mm probe using sample E to compare spinning a sample verses not spinning. Figure 4.34 shows the spectrum of a static sample E, while Figure 4.35 is showing a comparison of the sample E which was spun to the

static sample. The spun sample is shown on top, and the static sample is shown on the bottom. The aliphatic and methine peaks are present but very broad in the static sample spectrum. The aromatic is small and broad, and the carbonyl peak is not observable in the static sample.

A comparison of the two probes can be seen in Figure 4.36. Sample D was used to evaluate the different spectra produced by the 5 mm probe and the 7 mm probe. The top spectrum was collected from the 7 mm probe and was spun at 2.2 kHz; the bottom one was from the 5 mm probe and was spun at 4.8 kHz. Faster spinning generally narrows lines and reduces spinning sidebands. When comparing the two spectra, the 5 mm probe sample has fewer spinning sidebands from the faster spinning, but the lines are not narrower, the aliphatic and methine peaks are actually broader than data from the 7 mm probe. In a general comparison of all the spectra from both probes, spectra from the 5 mm probe reduces the spinning sidebands from the 7 mm probe spectra, but does not largely affect the peak width.

A sample of burnt hair was also analyzed. The hair used was from a donor (Dr. Tadashi Tokuhiro) and was heated to 350 °C for 16 minutes. Figure 4.37 shows the  $^{13}\text{C}$  CP/MAS spectrum obtained. The spectrum shows no distinct peaks, but small humps where the aliphatic, aromatic, and carbonyl peaks would be. It is possible that the process of burning converts the amino acids to just carbon atoms, while releasing oxygen, nitrogen, and hydrogen into the atmosphere.



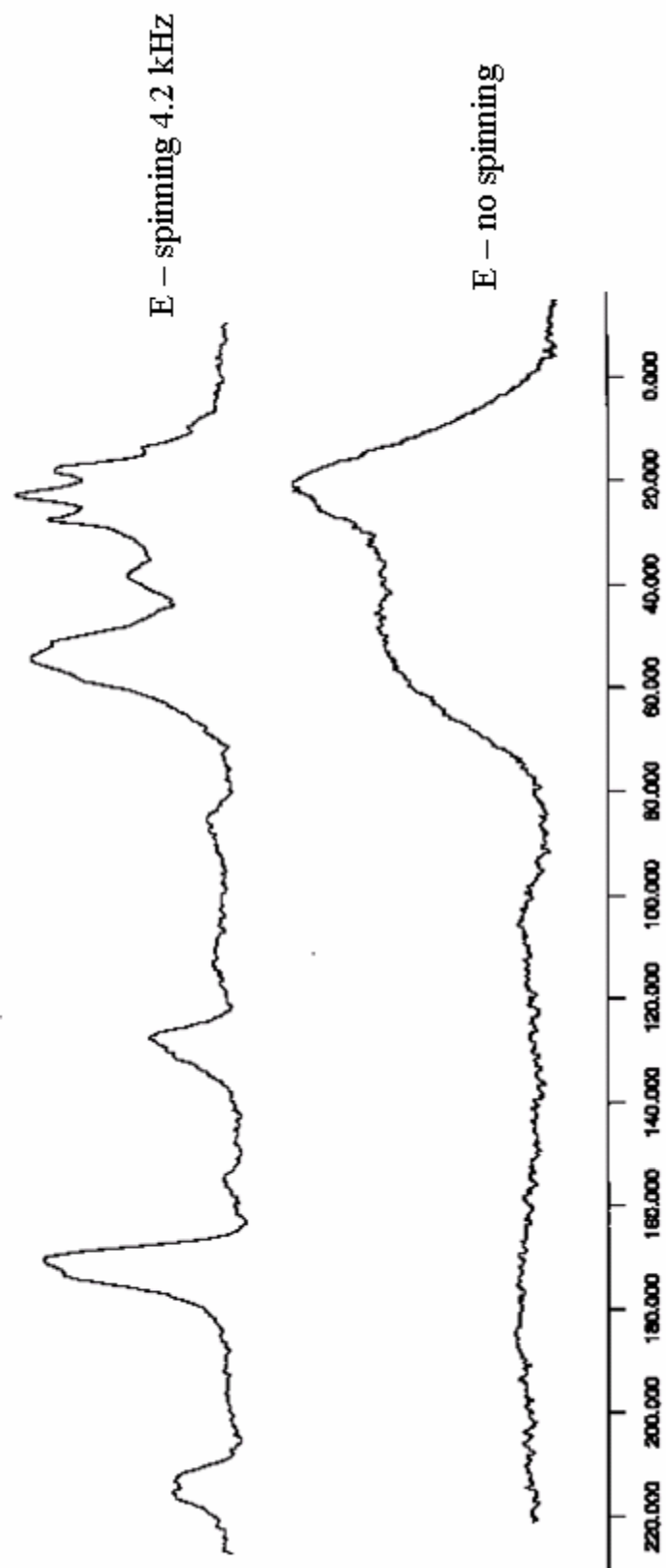


**Figure 4.35.** Comparison of sample E with spinning (top spectrum) and without spinning (bottom spectrum).

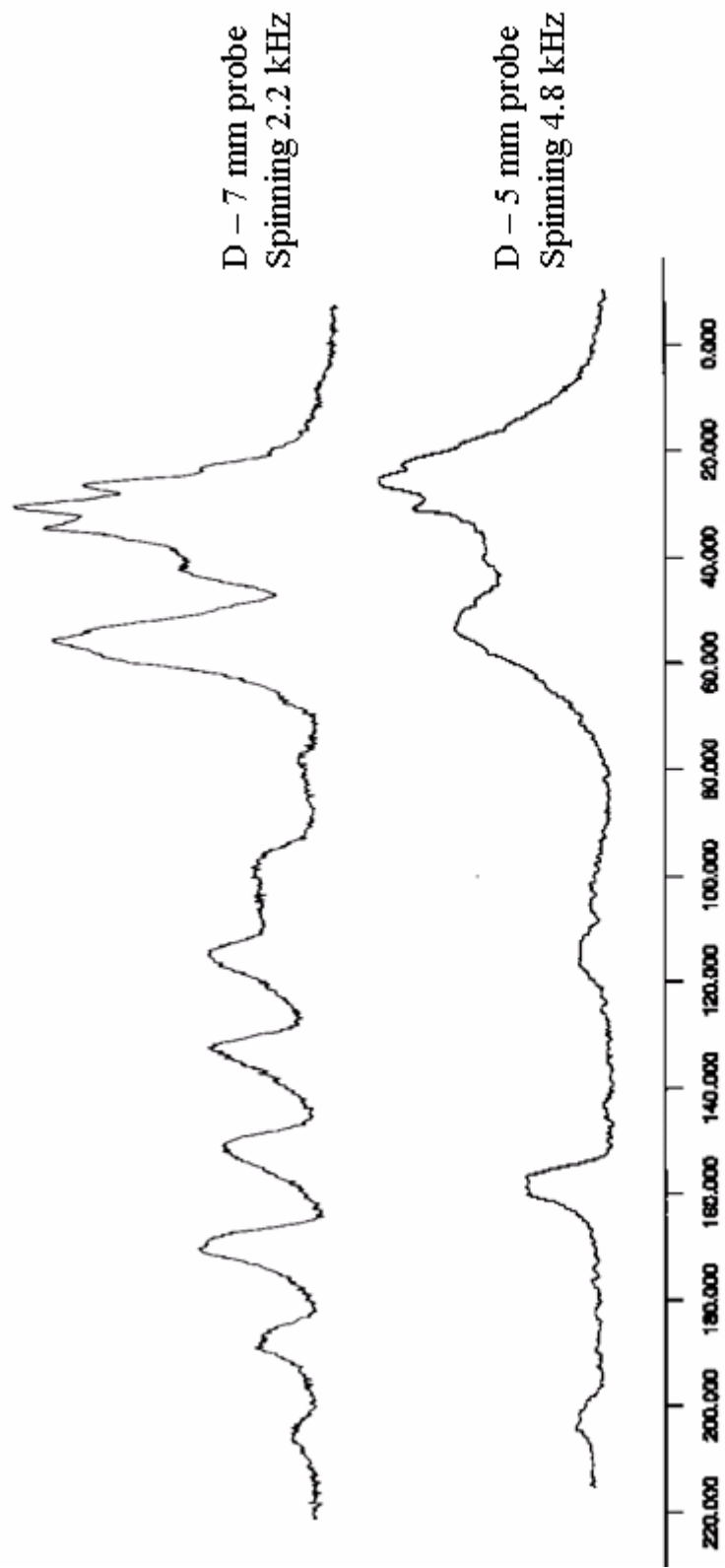


**Figure 4.36.** Comparison of the two probes using sample D. Top spectrum is the 7 mm probe and bottom spectrum is 5 mm probe.



## 5. DISCUSSION

### 5.1. DIFFERENTIAL SCANNING CALORIMETRY (DSC)

The DSC results showed a large endothermic peak at 155 °C and a second broad endothermic peak around 200 °C. Several investigations have been performed using DSC to study hair; however, the studies produced inconsistent results. One study looked at Merino wool (Wortmann et al., 1998). The thermogram yielded two endothermic peaks at 138 °C and 144 °C. These peaks were attributed to ortho- and para- cortical cells, respectively. The samples were run in water between 80-170 °C with a heating rate of 5 °C per minute. Sample sizes were 4-7 mg and 50 µl of water was used. The same group performed DSC studies in a dry environment, which yielded denaturation peaks at 230 °C and 240 °C, again corresponding to the ortho- and para- cortical cells. Another investigation of human hair with water using DSC yielded only one peak at 156.7 °C, corresponding to helix denaturation (Wortmann et al., 2002). The temperature range of this study was 50-190 °C with a heating rate of 10 °C per minute; the sample sizes were 4-7 mg with 50 µl of water. The difference in these two studies can possibly be explained by the heating rate. The first study (Wortmann et al., 1998) was heated at a slower rate of 5 °C per minute, compared to 10 °C per minute, which could cause peaks to appear at lower temperatures and also show more detail, explaining why there are two peaks compared to one peak reported by Wortmann et al. Although the first study examined Merino wool and the second used human hair, the differences between wool and human hair are very small, and a lot of research for human hair uses wool or other forms of protein such as hoof, horse hair, or feathers (Wortmann et al., 1998; Nishikawa et al., 1998; Yoshimizu et al., 1991; Duer et al., 2003; Thomas et al., 1986; Kricheldorf et al., 1984).

Additional research has been done on hair with DSC in an attempt to mimic the environment that hair is actually exposed to (Milczarek et al. 1992). These studies were performed by adding water to a pan and then puncturing the pan to allow the water to evaporate as it was heated, which mimics hair being dried or curled. They found that hair exposed to water exhibited a large water release peak around 70 °C, while hair which was allowed to anneal at temperatures above 100 °C did not exhibit that peak. They also

observed two different processes in the thermograms. One process at 155 °C was attributed to a transition in the amorphous phase, known as the “toughening transition,” and was not a peak but a change in slope which was described as an opposite character of  $T_g$ . The other process showed a peak at 233 °C due to the melting/denaturation of the  $\alpha$ -crystalline phase. The researchers pointed out that thermal transitions of keratin are greatly affected by water and the amount of water present.

Our studies examined the hair samples with water over a temperature range of 30-250 °C and were ramped 10 °C per minute. The sample sizes were roughly 10 mg of hair with 20 mg of water (on average). Our research yielded peaks at 155 °C and a broad peak at 200 °C presumably due to denaturation of cortical cells and denature of keratin, respectively. These peak assignments are based on the Wortmann et al. study and TGA analysis of the hair (Wortmann et al., 1998). It is assumed that the temperature of denaturation is dependent on the crosslink density of the matrix which surrounds the intermediate filaments. Knowing that cortical cells are amorphous and more weakly crosslinked than keratin, the peak at 155 °C is assumed to be the denaturing of cortical cells. Since keratin is the strongest component of hair and it is known through TGA research that keratin denatures at higher temperatures than cortical cells (Monteiro et al., 2005), the broad peak at 200 °C is probably due to keratin denaturation. Although the first two studies mentioned did not observe the broad peak around 200 °C, the temperatures probed only went up to 170 °C and 190 °C, so a peak at 200 °C would not have been visible. Earlier research stating that the amount of water strongly affected the thermal transitions of keratin (Milczarek et al., 1992) was not known during these trials and could possibly account for differences in the results since smaller amounts of water was used for our studies compared to previous work. The peak at 155 °C was very reproducible; however, the peak at 200 °C, while retaining a similar broad shape, did show variations. The variations could be due to different water amounts, as suggested by Milczarek et al. (Milczarek et al., 1992), or contamination of the DSC cell which happens due to pan rupture in cell.

## 5.2. THERMOGRAVIMETRIC ANALYSIS (TGA)

TGA analysis showed that the treated hair samples from lot 1 lost mass slower than the untreated sample. Other research performed by Monteiro et al. compared untreated hair to bleached and chlorinated hair (Monteiro et al., 2005). The treated samples exhibited fewer mass loss steps and at lower temperatures than the untreated hair. Their proposition for this is that the hair keratin becomes disorganized after the treatment, yet produces a uniform disorganization which shows fewer mass loss steps. Our research showed that the treated hair also lost mass slower, agreeing with their research, but the treated samples showed more mass loss steps than the untreated, contrary to their research.

One explanation for the variation in mass loss steps could be simply that the trials were done with hair from different individuals. It was shown in the results section (Figure 4.7) that hair samples exposed to the same treatments, yet from different individuals showed different mass loss temperatures and steps. Therefore, a treatment's affect may vary between hair samples from different people. To further confirm this, the treated hair from lot 2 lost mass faster than the untreated hair. Our research showed that untreated hair from different individuals has the same shape and mass loss steps, but it is the treated hair that can vary. An explanation for this is that hair samples from different people have variations in the resiliency to treatments, which can cause a difference in the disorganization of the hair matrix and keratin.

Instrumental or experimental differences between Monteiro's et al. research and our studies most likely do not account for the differences in the results. Their studies heated the sample at a rate of 3 K per minute from 25-720 °C compared to our experiments which were heated at 5 °C per minute from 30-750 °C (Monteiro et al., 2005). Although it was determined by our research that slower heating rates yielded more detail and reproducibility (Figures 4.3 and 4.4), the difference in heating rate is small and therefore negligible.

The mass loss steps can be assigned starting with an initial step from 25-130 °C due to loss of water, and then up to 400 °C the degradation of organic matter and denaturation of keratin takes place. The keratin degraded from 400-600 °C (Monteiro et al., 2005). Differences of the treated hair in the region from 500-600 °C were noticeable.

Treatment C lost mass the slowest, followed by treatments B and E, while treatment D retains a very similar shape to the untreated sample (A) but has a slightly rough line shape. The reason for this could be similar to the reason given by Monteiro et al. where the treatments cause disorganization of the keratin which changes the mass loss rates (Monteiro et al., 2005). Using this analogy, treatment C has the most disorganization of the keratin, followed by treatments B and E, and treatment D seems to be the least affected.

Another explanation as to why the treated samples lost mass slower than the untreated sample could be similar to the theory put forth by Humphries et al. In their studies, hair samples which were oxidized with  $H_2O_2$ , crosslinked with formaldehyde vapors, and supercontracted by heating to 95 °C in 8M LiBr, showed mass loss at higher temperatures than the untreated sample and the sample which was reduced with thioglycolic acid. Reducing hair converts disulfide crosslinks to thiol groups which are less thermally stable. Their reasoning for the higher temperature mass losses is that the crosslinked sample may have formed bridges between the polypeptide chains of which hair is made of, creating more structural support for the hair. For the supercontracted sample, shortening of the sample resulted in folding of the polypeptide chains and also leads to more thermal stability (Humphries et al., 1972). A description on the molecular level as to why the oxidized sample also exhibited an increased mass loss was not given. Although our samples may or may not have been exposed to the same treatments, a similar process could have taken place with our samples where bridging between polypeptides chains or folding of polypeptides chains created a more thermally stable hair structure. Using this reasoning, treatment C created the most structural change, followed by treatments B and E, and treatment D seems to be the least affected.

When taking into consideration the treatments and how they may have influenced the results, there are a few differences than the expected outcome. Treatment C, which is sodium hydroxide, is the most aggressive of the reducing agents analyzed and therefore should show the most disorganization of keratin. Treatment D, guanidine hydroxide, although a less aggressive reducing agent than sodium hydroxide, would be expected to affect the hair similarly to sodium hydroxide because of the comparable hydroxide technologies. Bleached treatment, sample E, is considered an aggressive oxidizing agent,

so a noticeable difference compared to the untreated hair would be expected.

Ammonium thioglycolate, sample B, is a less aggressive reducing agent, but showed a very similar mass loss trend as the bleached hair.

### **5.3. FOURIER TRANSFORM INFRARED SPECTROSCOPY (FTIR)**

Hair treatments and environmental weathering can cause the conversion of cystine to cysteic acid, cystine monoxide, and cystine dioxide as well as to sulfonates (Robbins, 2002; Strassburger et al., 1985). The FTIR results obtained in our studies showed that all the hair samples, including the untreated sample displayed these cystine derivatives. The spectra of the samples are shown in Figure 4.9. FTIR only penetrates the outer portion of hair which is the cuticle. Environmental weathering such as exposure to ozone can cause the oxidation products of cystine to form in the cuticle. It is possible to determine the amount of oxidative damage in a quantitative manner (Strassburger et al., 1985); however, we chose not to try it.

Early FTIR studies used attenuated total reflection (ATR) to compare bleached hair samples to untreated hair samples. (Atler et al., 1969) Their untreated hair showed peaks at 1040 and 1175  $\text{cm}^{-1}$  corresponding to cysteic acid and sulfonates, respectively presumably from environmental oxidation. After bleaching, the hair showed the presence of cystine dioxide at 1220  $\text{cm}^{-1}$  and increased sulfonates intensity at 1175  $\text{cm}^{-1}$ . However, the overall appearance of the bleached hair spectrum was not significantly different from the untreated hair spectrum.

Other FTIR studies of hair examined oxidative damage due to bleaching, permanent waving, and environmental exposure to hair with a high pressure diamond anvil cell (Strassburger et al., 1985). To quantify the amount of oxidative damage Strassburger et al. normalized the S=O band at 1040  $\text{cm}^{-1}$  and compared its intensities to the other band intensities. Several measurements were taken of each band and an average was reported. Although this method was determined to be reproducible, the coefficient of variation between each measurement was high. Their overall conclusions were that permanent waving was more destructive than bleaching.

In our studies the amount of oxidation was not determined in a quantitative manner. Peaks at 1075, 1175, and 1229  $\text{cm}^{-1}$  which corresponds to oxidative damage

were observed for all hair samples. A peak at  $1040\text{ cm}^{-1}$ , due to the S=O symmetrical stretch of sulfonate, was slightly observed for samples C and D, and was clearly observed in sample E. The appearance of this peak for sample E is due to the oxidizing nature of the bleaching treatment. Peaks at  $1241$ ,  $1454$ ,  $1550$ , and  $1655\text{ cm}^{-1}$  correspond to typical amino acid bands such as amide III (N-H stretch),  $\text{CH}_2$ , amide II (C-N stretch), and amide I (C=O stretch), respectively. For samples D and E, the intensity of both  $1550$  and  $1655\text{ cm}^{-1}$  increased compared to the other samples, possibly due to more amides present from breaking amino acid chains caused by the guanidine hydroxide and bleaching treatments. At higher frequency, two CH (aliphatic) peaks are observed for all samples at  $2885$  and  $2960\text{ cm}^{-1}$ . A broad hydroxyl peak due to water is clearly observed for all samples at  $3550\text{ cm}^{-1}$ . An additional broad peak appears at  $3315\text{ cm}^{-1}$  for samples C, D, and E, and may be due to a primary amine which may be present after the breaking of amino acid chains caused by sodium hydroxide, guanidine hydroxide, and bleaching treatments. Treatment B, ammonium thioglycolate, did not show distinct differences from the untreated sample, A, observable with FTIR. A comparison of our spectra to spectra obtained by other researcher's showed basic similarities, as far as peaks, observed (Atler et al., 1968; Strassburger et al., 1985).

Data obtained by FTIR maybe useful in determining if oxidation occurs during hair treatment processes if the untreated hair used for comparison has no oxidation from environmental factors. Other methods to obtain IR spectra (besides using KBr pellet) could be explored for more conclusive results, such as ATR IR which is commonly used to study the surface of a material.

#### **5.4. $^{13}\text{C}$ CROSS POLARIZATION/MAGIC ANGLE SPIN (CP/MAS) NMR**

Analysis of the hair samples with  $^{13}\text{C}$  CP/MAS NMR revealed slight differences of the peak shape. The data from the 5 mm probe was used to compare the peak shapes, with the exception of sample B where data from the 7 mm probe was used because of poor data from the 5 mm probe. Previous work by Nishikawa et al. compared untreated hair to hair which was exposed to various time periods of permanent waving treatments. Rather than analyzing the hair as individual amino acids, they analyzed according to the higher order structures of the helix, sheet, and coil proteins which compose the

microfibrils. They observed a difference in the shape of the carbonyl peaks after the treatments. The top of the carbonyl peak of the untreated hair was tilted slightly to lower frequency and a small hump was visible at higher frequency. After successive treatments of up to 180 minutes exposure time, the small hump at higher frequency was gone, although the peak remained tilted toward lower frequency. The small hump at higher frequency was at 176 ppm and is due to  $\alpha$ -helical proteins, while the larger hump at lower frequency is a combination of random coils and  $\beta$ -sheet structure proteins. They suggested that treatments caused  $\alpha$ -helix structures to convert to random coils. This group also observed differences in the aliphatic,  $C^\alpha$  methine, and aromatic peaks, but chose the carbonyl peak for study (Nishikawa et al., 1998 – a).

A closer comparison of the carbonyl peaks from our research, as seen in Figure 5.1, showed untreated hair with the same shape as the untreated from Nishikawa's et al. research, the peak slightly leaning toward lower frequency with a small hump at higher frequency. After treatments, the small hump at higher frequency decreased in intensity, suggesting that  $\alpha$ -helix structures in the hair were converted to random coils because of the treatments. Sample C changed the most from the untreated sample, exhibiting overall small intensity of the carbonyl peak and a flatter top than the rest of the samples. Samples B and E still had the appearance of a small hump at higher frequency, while sample D had a mostly smooth left side. Using the assessment given by Nishikawa's et al. research of  $\alpha$ -helix structures converting to random coils when exposed to treatments, treatment C changes the hair's organized  $\alpha$ -helix structures the most, followed by sample D, E, and B changing the least from the untreated sample, A. These observations are similar to the predicated outcome. Sodium hydroxide, sample C, being the most aggressive reducing agent, exhibited the most change. Guanidine hydroxide, sample D, being a similar treatment to sodium hydroxide, showed the second largest amount of change. Close in amount of change to sample D was sample E, bleaching, which is an aggressive oxidizing agent. Ammonium thioglycolate, sample B, which showed the least amount of change, is a less aggressive treatment compared to the other treatments.

To assess the differences of the aliphatic and methine peaks, Figure 5.2 shows a close-up of the aliphatic region of the spectra for samples A - E. The aliphatic peaks mostly consist of Ile, Leu, Ala, Val, Pro, Lys, Arg, and Thr amino acids. The methine

peak consists of Phe, Tyr, Ser, Thr, Asp, Glu, Leu, and Cys amino acids, among others. The amino acids listed are a general composition and can vary between individuals. A close comparison of the spectra reveals that samples A, C, and E have very similar aliphatic peaks. The differences in these spectra could be due to a couple reasons. The data for sample B is from the 7 mm probe, where the other samples are from the 5 mm probe and spun at higher speeds, which can give slightly different shaped peaks. Sample D was spun at the slowest speed compared to the other samples in the 5 mm probe, which could account for poor spectra results.

The methine peaks for sample A, B, and E were similar, with a larger peak in the middle and two smaller peaks on each side. Sample D is different, but probably for the same reason as the aliphatic peak difference, slower spinning so poor results. Sample C is different in that the methine peak has a larger peak to the left than the other samples. An assessment of the aromatic peaks from Figure 4.32 can be done by a basic comparison because spinning sidebands are in the same region as the aromatic peaks. The aromatic region is from 115-158 ppm and the amino acids involved are Phe, Tyr, and Trp, and each are found in very small or nonexistent quantities in hair. Sample A, the untreated sample, had small aromatic activity from 110-120 ppm and also around 155 ppm. Samples B and E showed the same trait, and sample D exhibited smaller aromatic peaks in the same area. Sample C was difficult to assess because of the spinning sidebands, but there probably is not an aromatic peak right next to the carbonyl, like the other samples but there may be one in the 110-120 ppm region. Overall, sample C, sodium hydroxide, the most aggressive reducing agent, showed the most difference from the untreated sample when comparing the carbonyl, methine, and aromatic peaks.

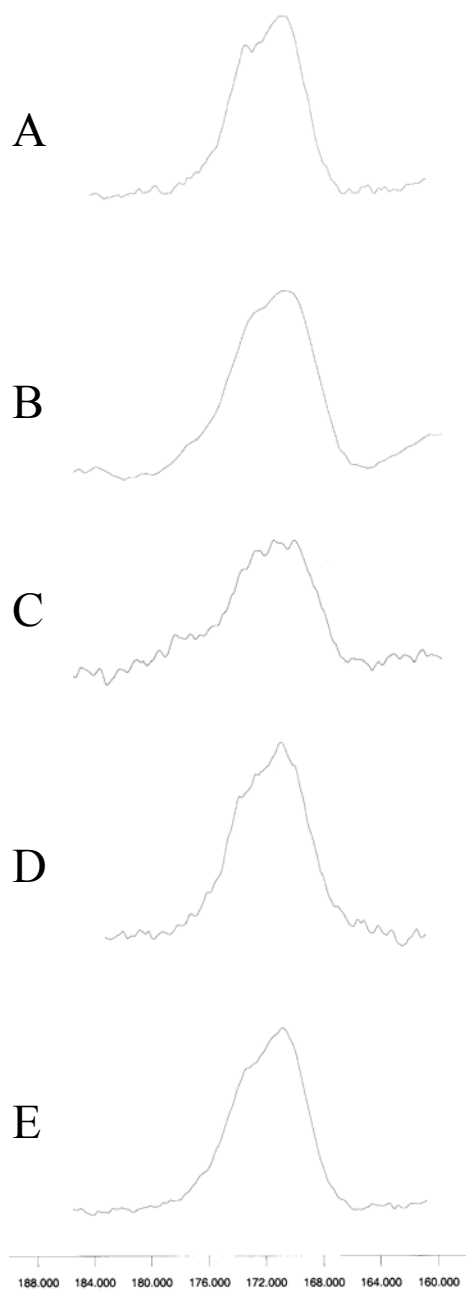


**Figure 5.1.** A close comparison of the carbonyl peaks for all samples. All spectra are from the 5 mm probe, with the exception of sample B which is from the 7 mm probe.

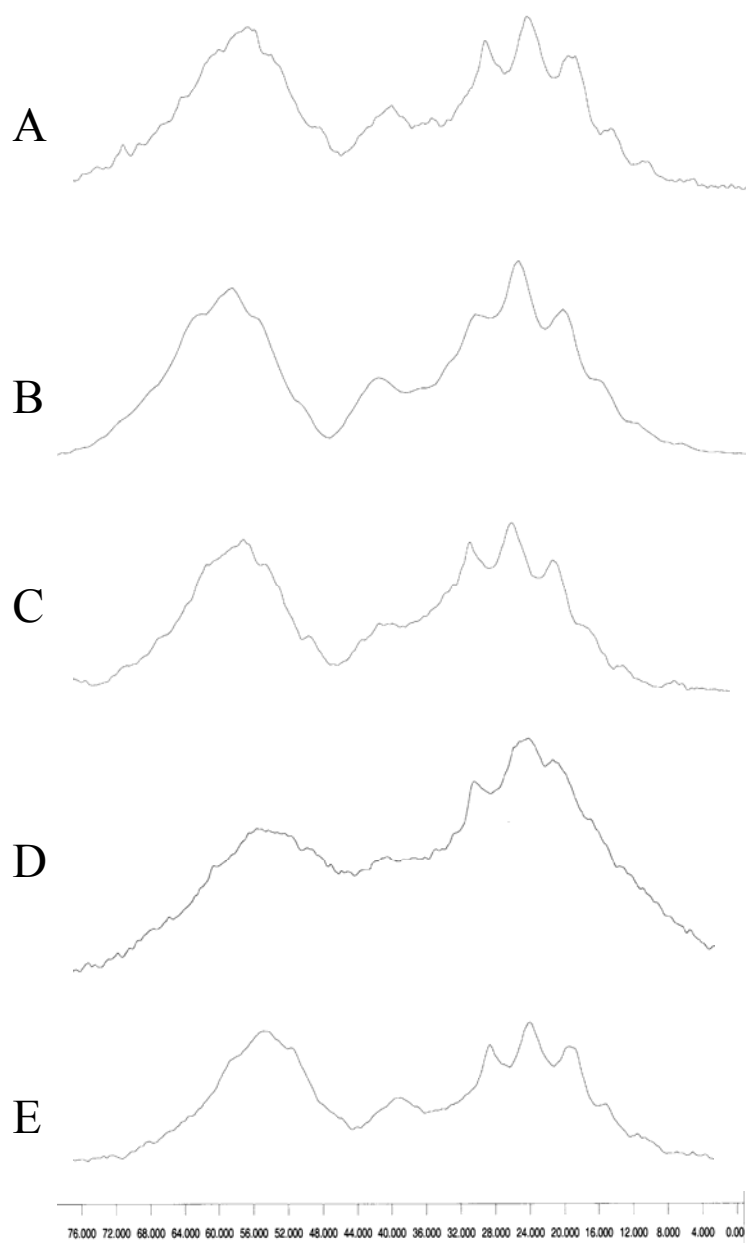


**Figure 5.2.** A close comparison of the aliphatic and methine peaks for all samples. All spectra are from the 5 mm probe, with the exception of sample B which is from the 7 mm probe.

## 6. CONCLUSIONS

Five hair samples were analyzed with various instrumental techniques. DSC results of the untreated hair sample yielded a thermogram with a peak at 155 °C due to denaturation of cortical cells and a broad peak at 200 °C due to the denaturation of keratin. This thermogram is comparable to results obtained by other researchers. The small differences between our results and results obtained by other researchers are probably due to the amount of water used for each sample, the heating rate, or the temperature range. TGA analysis showed a mass loss variation in the range of 500-600 °C for the treated samples compared to the untreated sample. The treated samples lost mass slower than the untreated sample. The reason for this could be either that the disorganization of the keratin simply creates a more stable structure, or the treatments caused bridges between or folding of polypeptide protein chains, also making a more thermally stable structure. In any case, treatment C showed the largest change, followed by treatments B and E, and treatment D was the least affected. This is somewhat contrary to the expected results. Treatment C, sodium hydroxide is considered to be the most aggressive, but treatment D, guanidine hydroxide is considered similar to sodium hydroxide and should therefore show the second largest amount of change rather than treatment B, ammonium thioglycolate, a less aggressive reducing agent, or treatment E, bleaching, an aggressive oxidizing agent.

FTIR analysis showed that oxidative damage was present in all the samples including the untreated sample. However, a peak appearance at 1040  $\text{cm}^{-1}$  due to sulfonates for samples C, D, and E (with E being the most intense) indicated that the treatments added oxidation products to the hair samples. Sample E, bleaching, an aggressive oxidizing agent, would be expected to exhibit the most intense peaks for oxidizing byproducts, such as sulfonates. Other differences between the samples include more intense amide peaks at 1550 and 1655  $\text{cm}^{-1}$  for samples D and E and the appearance of a primary amine peak at 3315  $\text{cm}^{-1}$  for samples C, D, and E. The differences could be due to breaking of amino acid chains after treatments, causing more amides and primary amines to be observed. Although the amount of oxidation was not quantified, sample E showed the most oxidation, with samples C, D, and E changing the most compared to the

untreated sample A. Samples C and D, sodium hydroxide and guanidine hydroxide are similar treatments and should have similar spectra, as shown. Sample B, ammonium thioglycolate, changed the least compared to the other treatments, which is to be expected because it is the least aggressive treatment.

The CP/MAS NMR data revealed differences in carbonyl peak shapes presumably due to  $\alpha$ -helical proteins converting to random coiled proteins after treatment. Treatment C changed the hair's organized  $\alpha$  - helix structures the most, followed by sample D, E, and B changing the least from the untreated sample, A. Slight changes in aliphatic, methine, and aromatic peaks were also observed, but were not large enough to determine which sample changed the most because spinning speed or other experimental differences could account for the slight differences. An overall comparison of the results obtained from each instrument, suggest that treatment C changed the most in comparison to the untreated sample A, followed by treatments D, E, and finally B. These results are similar to the predicted results because treatment C is the most aggressive reducing agent tested. Treatment D (guanidine hydroxide) is similar to treatment C (sodium hydroxide), and treatment E (bleached) is more aggressive than treatment B (ammonium thioglycolate).

This work was important to understand the changes of the hair structure after various treatments. Although the treatments analyzed were common treatments, this information may provide more insight into how hair changes on the molecular level, which in turn may lead to better treatment formulations or procedures which could potentially perform a certain task with minimal negative damage to the hair.

**BIBLIOGRAPHY**

Adhyaru, B. B.; Akhmedov, N. G.; Katritzky, A. R.; Bowers, C. R. *Magnetic Resonance in Chemistry*, **2003**, *41*, 466.

Atler, Harvey; Bit-Alkhas, Michael. *Textile Research Journal*, **1969**, *39*, 479.

Benitez, J. J.; Matas, A. J.; Heredia, A. *Journal of Structural Biology*, **2004**, *147*, 179.

Bilinska, B.; Kolczynska-Szafraniec, U.; Buszman, E. *Postepy Fizyki Medycznej*, **1991**, *26*, 75.

Braun, S., Kalinowski, H.-O., Berger S., *150 and More Basic NMR Experiments*, Wiley, Weinheim, Germany, 1998.

Caldwell, E. S. (1996) An investigation of chemical hair straighteners, M.S. Thesis, University of Cincinnati.

Chan, K. L. A.; Kazarian, S. G.; Mavraki, A.; Williams, D. R. *Applied Spectroscopy*, **2005**, *59*, 149.

Clifford, J.; Sheard, B. *Biopolymers*, **1966**, *4*, 1057.

Éhen, Zs.; Novák, Cs.; Sztatisz, J.; Bene, O. *Journal of Thermal Analysis and Calorimetry*, **2004**, *78*, 427.

Derome, A. E.; Bowden, S. *Chemical Reviews*, **1991**, *91*, 1307.

Duer, Melinda J.; McDougal, Nicky; Murray, Rachel C. *Physical Chemistry Chemical Physics*, **2003**, *5*, 2894.

Fyfe, Colin A., *Solid State NMR for Chemists.*, C.F.C Press, Ontario, Canada, 1983.

Gniadecka, M.; Nielson, O. F.; Christensen, D. H.; Wulf, H. C. *Journal of Investigative Dermatology*, **1998**, *110*, 393.

Humphries, W.T.; Miller, D.L.; Wildnauer, R.H. *Journal of the Society of Cosmetic Chemists*, **1972**, *23*, 359.

Ionashiro, E.Y.; Hewer, T.S.R.; Fertoni, F.L.; de Almeida, E.T.; Ionashiro, M. *Eclética Química*, **2004**, *29*, 53.

Itou, T.; Masayoshi, N.; Ootsuka, Y.; Nakamura, K.; *Journal of Cosmetic Science*, **2006**, *57*, 139.

- Kirschenbaum, L. J.; Coutinho, L.; Huffman, S. W.; Brown, C. *Abstract of Papers*, **2000**.
- Kricheldorf, H.R.; Müller, D. *Colloid and Polymer Science*, **1984**, 262, 856.
- Lindberg, J. J.; Hortling, B.; Martinmaa, J. *Teubner-Texte zur Physik*, **1986**, 9, 229.
- Liu, Y.; Hong, L.; Wakamatsu, K.; Ito, S.; Adhyaru, B.; Cheng, C.-Y.; Bowers, C. R.; Simon, J. D. *Photochemistry and Photobiology*, **2005**, 81, 135.
- Lyman, D. J.; Murray-Wijelath, J.; Feughelman, M. *Applied Spectroscopy*, **2001**, 55, 552.
- Martin, Kathleen. *The Internet Journal of Vibrational Spectroscopy*, **1999**, 3(2), 1.
- Milczarek, P.; Zielinski, M.; Garcia, M.L. *Colloid and Polymer Science*, **1992**, 270, 1106.
- Miyamae, Y.; Yamakawa, Y.; Ozaki, Y. *IFSCC Magazine*, **2006**, 9, 219.
- Monteiro, Valéria F.; Maciel, A.P.; Longo, E. *Journal of Thermal Analysis and Calorimetry*, **2005**, 79, 289.
- Morinaga, H.; Ochiai, B.; Mori, H.; Endo, T. *Journal of Polymer Science: Part A: Polymer Chemistry*, **2006**, 44, 3778.
- Nishikawa, Naoki; Tanizawa, Yoshiaki; Tanaka, Shoichi; Horiguchi, Yasunobu; Asakura, Tetsuo. *Polymer*, **1998**, 39, 3835 (a).
- Nishikawa, Naoki; Tanizawa, Yoshiaki; Tanaka, Shoichi; Horiguchi, Yasunobu; Matsuno, Hitomi; Asakura, Tetsuo. *Polymer Journal*, **1998**, 30, 125 (b).
- Popescu, C.; Wortmann, F.-J. *Revue Roumaine de Chimie*, **2003**, 48, 981.
- Quadflieg, J. M. (2003) Fundamental properties of Afro-American hair as related to their straightening, relaxing behaviour, Ph.D thesis, RWTH Aachen University.
- Robbins, Clarence R., *Chemical and Physical Behavior of Human Hair, 4th Ed.*, Springer, New York, 2002.
- Signori, Vittoria; Lewis, David M. *Macromolecule Symposium*, **1997**, 119, 235.
- Silverstein, Robert M.; Bassler, G. Clayton; Morrill, Terence C., *Spectrometric Identification of Organic Compounds, 4<sup>th</sup> Ed.*, Wiley, New York, 1981.
- Smith, S. O.; Griffin, R. G. *Annual Review of Physical Chemistry*, **1988**, 39, 511.
- Stevens, Malcolm P., *Polymer Chemistry, 3<sup>rd</sup> Ed.*, Oxford, New York, 1999.

Strassburger, John; Breuer, Miklos M. *Journal of the Society of Cosmetic Chemists*, **1985**, 36, 61.

Thomas, Helga; Conrads, Andrea; Phan, Kim-Hô; van de Löcht, Monika; Zahn, Helmut. *International Journal of Biological Macromolecules*, **1986**, 8, 258.

Witteler, H.; Blum, R.; Hossel, P.; Sanner, A.; Schwalm, R.; Dausch, W. M.; Jaworek, T.; Koniger, R. *European Patent Application*, **2001**, EP 1116484.

Wortmann, F.-J.; Deutz, H., *Journal of Applied Polymer Science*, **1998**, 68, 1991.

Wortmann, F.-J.; Springbob, C.; Sendelbach, G. *Journal of Cosmetic Science*, **2002**, 53, 219.

Wortmann, F.-J.; Stapels, M.; Elliott, R.; Chandra, L. *Biopolymers*, **2006**, 81, 371.

Yoshimizu, Hiroaki; Mimura, Hiroyuki; Ando, Isao. *Macromolecules*, **1991**, 24, 862.

## VITA

Lea Marie Dankers was born in Cambridge, Minnesota on May 24<sup>th</sup>, 1983. She finished her BS in chemistry at the University of Wisconsin – River Falls in River Falls, WI in May of 2005. Lea joined the University of Missouri – Rolla chemistry department in August of 2005 where she started working for Frank D. Blum studying human hair.